

DLR-IB-FT-BS-2022-38

**Development of an energy-based
speed envelope for increased
glideslope angles**

Internal Report

Authors: Dennis Vechtel, Peter Pauly



DLR

**Deutsches Zentrum
für Luft- und Raumfahrt**

Institute Report
DLR-IB-FT-BS-2022/38

**Development of an energy-based speed
envelope for increased glideslope angles**

D. Vechtel
P. Pauly

Institute of Flight Systems
Braunschweig

50 Pages
33 Figures
3 References

German Aerospace Center (DLR)
Institute of Flight Systems
Department Flight Dynamics and Simulation

Level of Accessibility: I, internally and externally unlimited distribution

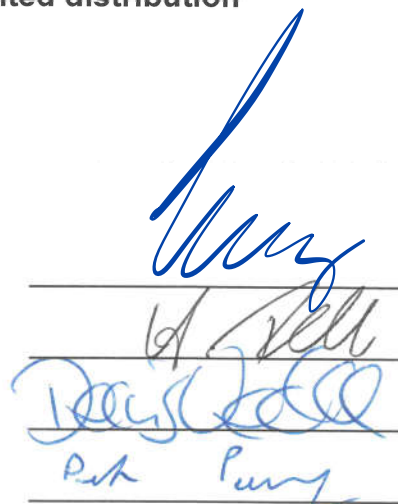
Braunschweig, July, 31st, 2022

Institute Director: Prof. Dr.-Ing. S. Levedag

Department Head: Dr.-Ing. H. Duda

Authors: Dr.-Ing. D. Vechtel

P. Pauly, M. Sc.



Four handwritten signatures in blue ink, each placed above a horizontal line. From top to bottom, the signatures correspond to Prof. Dr.-Ing. S. Levedag, Dr.-Ing. H. Duda, Dr.-Ing. D. Vechtel, and P. Pauly.



Intentionally left blank

Content

LIST OF REVISIONS	4
TABLE OF FIGURES.....	5
NOMENCLATURE	7
1 INTRODUCTION	9
2 METHODOLOGY	10
2.1 PROGRAM SEQUENCE.....	10
2.2 CALCULATIONS PER TIMESTEP	11
2.2.1 Stabilised approach segment	11
2.2.2 Flap deployment segment	12
2.2.3 Segment without flap transition.....	15
2.2.4 Gear deployment segment	15
2.2.5 Aerodynamics during gear and flap deployment	16
2.3 COMPLETE APPROACH CALCULATIONS.....	16
2.4 GRAPHICAL DEPICTION OF THE ENVELOPE	17
3 VERIFICATION.....	20
3.1 COMPARISON TO REAL FLIGHT DATA	20
3.1.1 A320.....	21
3.1.2 B737-800	24
3.2 VARIATION OF AIRCRAFT PERFORMANCE MODELS	28
4 RESULTS FOR DIFFERENT AIRCRAFT TYPES.....	31
4.1 AIRBUS A319.....	31
4.2 AIRBUS A320.....	36
4.3 AIRBUS A321.....	38
4.4 AIRBUS A320 FAMILY COMPARISON.....	41
4.5 BOEING B787-9.....	42
4.6 INFLUENCE ON FUEL CONSUMPTION AND NOISE	44
4.7 BUSINESS JET.....	47
5 CONCLUSIONS	48
6 REFERENCES	50

Table of Figures

FIGURE 1: EXEMPLARY APPROACH WITH LOWEST AND HIGHEST GLIDEPATH INTERCEPT SPEED (TRIMMED POLAR MODEL).....	16
FIGURE 2: EXEMPLARY DEPICTION OF THE SPEED ENVELOPE (TRIMMED POLAR MODEL).....	18
FIGURE 3: EXEMPLARY DEPICTION OF THE CONFIGURATION ALTITUDES (TRIMMED POLAR MODEL).....	19
FIGURE 4: FIT OF BACKWARDS SIMULATION AND FLIGHT DATA OF A320 WITH TRIMMED POLAR MODEL (3° GLIDESLOPE ANGLE).....	21
FIGURE 5: FIT OF BACKWARDS SIMULATION AND FLIGHT DATA OF A320 WITH TRIMMED POLAR MODEL (3° GLIDESLOPE ANGLE).....	22
FIGURE 6: FIT OF BACKWARDS SIMULATION AND FLIGHT DATA OF A320 WITH TRIMMED POLAR MODEL (3.2° GLIDESLOPE ANGLE).....	23
FIGURE 7: COMPARISON OF BACKWARDS SIMULATION AND FLIGHT DATA OF A320 WITH TRIMMED POLAR MODEL AND ANP MODEL (3.2° GLIDESLOPE ANGLE).....	23
FIGURE 8: FIT OF BACKWARDS SIMULATION AND FLIGHT DATA OF B737-800 WITH ORIGINAL ANP MODEL (3° GLIDESLOPE ANGLE).....	25
FIGURE 9: FIT OF BACKWARDS SIMULATION AND FLIGHT DATA OF B737-800 WITH ORIGINAL ANP MODEL (3° GLIDESLOPE ANGLE).....	25
FIGURE 10: FIT OF BACKWARDS SIMULATION AND FLIGHT DATA OF B737-800 WITH ORIGINAL ANP MODEL (3° GLIDESLOPE ANGLE).....	26
FIGURE 11: FIT OF BACKWARDS SIMULATION AND FLIGHT DATA OF B737-800 WITH ADAPTED ANP MODEL (3° GLIDESLOPE ANGLE) – SAME FLIGHT AS IN FIGURE 8.....	27
FIGURE 12: FIT OF BACKWARDS SIMULATION AND FLIGHT DATA OF B737-800 WITH ADAPTED ANP MODEL (3° GLIDESLOPE ANGLE) – SAME FLIGHT AS IN FIGURE 9.....	27
FIGURE 13: FIT OF BACKWARDS SIMULATION AND FLIGHT DATA OF B737-800 WITH ADAPTED ANP MODEL (3° GLIDESLOPE ANGLE) – SAME FLIGHT AS IN FIGURE 10.....	28
FIGURE 14: COMPARISON OF TRIMMED POLAR MODEL AND ANP FOR A320 WITH 55 T AND NO WIND (LEFT: HIGHEST SPEED INTERCEPT; RIGHT: LOWEST SPEED INTERCEPT).....	29
FIGURE 15: INFLUENCE OF THE USED MODEL ON THE SPEED ENVELOPE (A320, AIRCRAFT MASS 55 T, INTERCEPT ALTITUDE 3,000 FT, NO WIND).....	30
FIGURE 16: INFLUENCE OF AIRCRAFT MASS ON SPEED ENVELOPE FOR A319 (INTERCEPT ALTITUDE 3,000 FT, NO WIND).....	31
FIGURE 17: INFLUENCE OF INTERCEPT ALTITUDE ON SPEED ENVELOPE FOR A319 (AIRCRAFT MASS 55 T, NO WIND).....	32
FIGURE 18: INFLUENCE OF HEADWIND COMPONENT ON SPEED ENVELOPE FOR A319 (AIRCRAFT MASS 55 T, INTERCEPT ALTITUDE 3,000 FT) – INTERCEPT WITH CONFIG2 ONLY.....	34
FIGURE 19: INFLUENCE OF HEADWIND COMPONENT ON SPEED ENVELOPE FOR A319 (AIRCRAFT MASS 55 T, INTERCEPT ALTITUDE 3,000 FT) – INTERCEPT WITH CONFIG1 AND CONFIG2.....	35
FIGURE 20: INFLUENCE OF THE AIRCRAFT MASS ON THE SPEED ENVELOPE FOR A320 (INTERCEPT ALTITUDE 3,000 FT, NO WIND).....	36
FIGURE 21: INFLUENCE OF THE INTERCEPT ALTITUDE ON THE SPEED ENVELOPE FOR A320 (AIRCRAFT MASS 55 T, NO WIND).....	37
FIGURE 22: INFLUENCE OF THE WIND ON THE SPEED ENVELOPE FOR A320 (AIRCRAFT MASS 55 T, INTERCEPT ALTITUDE 3,000 FT) – INTERCEPT WITH CONFIG2 ONLY.....	37
FIGURE 23: INFLUENCE OF THE WIND ON THE SPEED ENVELOPE FOR A320 (AIRCRAFT MASS 55 T, INTERCEPT ALTITUDE 3,000 FT) – INTERCEPT WITH CONFIG1 AND CONFIG2.....	38
FIGURE 24: INFLUENCE OF THE AIRCRAFT MASS ON THE SPEED ENVELOPE FOR A321 (INTERCEPT ALTITUDE 3,000 FT, NO WIND).....	39
FIGURE 25: INFLUENCE OF THE INTERCEPT ALTITUDE ON THE SPEED ENVELOPE FOR A321 (AIRCRAFT MASS 65 T, NO WIND).....	40
FIGURE 26: INFLUENCE OF THE WIND ON THE SPEED ENVELOPE FOR A321 (AIRCRAFT MASS 65 T, INTERCEPT ALTITUDE 3,000 FT) – INTERCEPT WITH CONFIG2 ONLY.....	40
FIGURE 27: INFLUENCE OF THE WIND ON THE SPEED ENVELOPE FOR A321 (AIRCRAFT MASS 65 T, INTERCEPT ALTITUDE 3,000 FT) – INTERCEPT WITH CONFIG1 AND CONFIG2.....	41
FIGURE 28: COMPARISON OF A320 FAMILY AT SAME CONDITIONS (AIRCRAFT MASS 60 T, INTERCEPT ALTITUDE 3,000 FT, NO WIND).....	42
FIGURE 29: INFLUENCE OF THE AIRCRAFT MASS ON THE SPEED ENVELOPE FOR B787-9 (INTERCEPT ALTITUDE 3,000 FT, NO WIND).....	43



FIGURE 30: INFLUENCE OF THE INTERCEPT ALTITUDE ON THE SPEED ENVELOPE FOR B787-9 (AIRCRAFT MASS 160 T, NO WIND). 43

FIGURE 31: INFLUENCE OF THE WIND ON THE SPEED ENVELOPE FOR B787-9 (AIRCRAFT MASS 160 T, INTERCEPT ALTITUDE 3,000 FT). 44

FIGURE 32: FUEL CONSUMPTION DURING FINAL APPROACH WITHIN THE ENERGY ENVELOPE (A320, AIRCRAFT MASS 55 T, INTERCEPT ALTITUDE 3,000 FT, NO WIND). 45

FIGURE 33: EXEMPLARY APPROACH FROM TOP OF DESCENT WITH LOWEST AND HIGHEST GLIDEPATH INTERCEPT SPEED (A320, AIRCRAFT MASS 55 T, INTERCEPT ALTITUDE 3,000 FT, NO WIND)..... 46

Nomenclature

Symbol	Unit	Description
a	m/s	speed of sound
Alt	m	altitude
C_D	-	drag coefficient
C_L	-	lift coefficient
$Dist$	NM	distance to threshold
g	m/s ²	gravitational acceleration
m	kg	mass
Ma	-	Mach number
n_{eng}	-	number of engines
S	m ²	wing area
t	s	time
T_{eng}	N	thrust per engine
V	m/s	velocity
γ	°	flight path angle
ρ	kg/m ³	air density
ρ_0	kg/m ³	air density at sea level

Index	Description
CAS	calibrated airspeed
GS	ground speed
TAS	true airspeed

Abbreviation	Description
ANP	Aircraft Noise and Performance database
GPA	Glide Path Angle
PFD	Primary Flight Display



Intentionally left blank

1 Introduction

This report was prepared in the framework of the SESAR project VLD1-W2 DREAMS (Grant 874469). Distribution and publication of content from this report must be approved by the authors in advance.

In order to tackle aviation's future challenges, aircraft need to fly as energy-efficient as possible. This does not only comprise technical development but also operational means, by which the energy efficiency of the aircraft can be increased through avoiding unnecessary waste of energy. Such operational means can be applied already with today's aircraft and can thus immediately increase the energy efficiency of today's aircraft without extensive technical changes. On the other hand, the further reduction of noise immissions of aircraft in the vicinity of airports is another important factor for future aviation. Increased glideslope angles during final approach are one operational means to reduce the noise immissions from aircraft. However, the increase of the glideslope angle must not negatively affect the aircraft's ability to fly energy-efficiently.

Within the above-mentioned SESAR project VLD1-W2 DREAMS energy-based speed envelopes have been developed and assessed for different aircraft types with increased glideslope angles. This evaluation shall give indications for flight physical limitations and influencing parameters, which should be considered when increased glideslope angles are planned at specific airports. The main focus of the work presented here are typical airline operations with modern transport aircraft types.

2 Methodology

The basic idea behind the evaluation of the energy-based envelope is a calculation of the approach in backwards direction from the touch-down point on the runway up to the glideslope intercept and further backwards. The approach is divided into different segments mainly described by the corresponding aircraft configuration in terms of flap settings and gear deployment.

The evaluation of the drag coefficient and idle thrust is based on different aircraft performance models. The models used here for the evaluation are

- an aircraft performance model which generates drag polars for trimmed flight as a function of the aircraft configuration, the lift coefficient and the Mach number – hereafter denoted as “trimmed polar model”, and
- the Aircraft Noise and Performance Database (ANP) provided by the Eurocontrol Experimental Centre [2] – hereafter denoted as “ANP”. The drawback of this performance model is that the aerodynamics are represented by a single lift-to-drag-ratio for each flap setting, meaning linear characteristics of the drag. This means that the model is only valid for specific points in the flight regime. The further away from this valid point a specific flight point is, the less accurate is the outcome of the calculation. For this reason, the ANP model is only used here in case that no other “trimmed polar model” is available for a specific aircraft.

2.1 Program sequence

As the approach is calculated backwards the sequence of approach segments described in the following is described in the opposite order, too. For reasons of simplification the following description is given for Airbus approach procedures. For aircraft types other than Airbus the sequence might be slightly different. However, the main idea remains the same.

The reader should be aware that in the following often the term “after” means in the logical sequence of the backwards calculation. In the real sequence of the approach this means “before”. For example, flaps configuration CONFIG 3 is always after CONFIG 2 in the real approach, whereas in the backwards calculation sequence the CONFIG 3 segment is calculated before the CONFIG 2 segment.

The backwards simulation of the approach starts with the touchdown on the runway with final approach speed and in final configuration. The following segment is the stabilised approach flown with constant final approach speed and final configuration from a stabilisation altitude (typically 1,000 ft agl.) down to the runway. Following to this, the segments with the deployment of CONFIG Full and the deceleration to final approach speed as well as the deployment of CONFIG 3 and deceleration to F-Speed is calculated. The deployment of CONFIG 3 and CONFIG Full is always

clustered together. The final configuration can be chosen to be CONFIG 3. In this case the stabilised approach is calculated with CONFIG 3 instead of CONFIG Full and the CONFIG Full segment is not executed. After the segment with deployment of CONFIG 3 a segment in CONFIG 2 and with gear down is calculated over a user-defined distance in nautical miles. After this, the segment with the gear deployment follows. Please note, that if the user defines the previous segment with CONFIG 2 and gear down with zero nautical miles the landing gear is deployed right before the segment with deployment of flap CONFIG 3. Following to the landing gear deployment a segment with flap deployment to CONFIG 2 and gear up with deceleration F-Speed is calculated. The last flap segment is that with flap deployment to CONFIG 1 and gear up while decelerating to S-Speed. The very last calculated segment is in clean configuration decelerating from 250 kts indicated airspeed to green dot speed.

If the aircraft reaches the user-defined glideslope intercept altitude in one of the aforementioned segments the aircraft flies horizontally from that point on (please, remind the backwards direction of the calculation).

In order to vary the speed at which the aircraft intercepts the glideslope the target speeds of each flap configuration can be varied. The lowest target speeds are the respective speeds as indicated to the pilot on the PFD. The highest target speed is the maximum speed (V_{FE}) of the respective following flap configuration. For example, the minimum target speed for the CONFIG 2 segment is the F-Speed, the maximum target speed is the V_{FE} of CONFIG 2.

2.2 Calculations per timestep

The calculation at each timestep is performed for individual aircraft configuration segments. At the start of each new segment the length of data already calculated is evaluated and the calculation of the new segment is initiated starting from here. This way, no fixed order in the sequence of segments exists and different segments can be combined arbitrarily without the need to adopt the counting of timesteps within the segments.

2.2.1 Stabilised approach segment

The segment that is calculated first is the stabilised approach segment. Here, the aircraft flies with fixed final approach speed from the stabilisation altitude (typically 1,000 ft agl.) down to the touchdown on the runway. Hence, the backwards calculation starts with the touchdown and calculates each timestep until reaching the stabilisation altitude. Please note, that the stabilised approach segment is flown with a constant calibrated airspeed, for which reason the true airspeed slightly changes. As the segment is flown with constant speed, no aerodynamics or thrust need to be evaluated and only the position of the aircraft needs to be evaluated given the approach speed and the glidepath angle *GPA*.

The distance to the touchdown point on the runway at each timestep $Dist(t_i)$ is a pure summation of the flown distance above ground using the ground speed V_{GS} and the step-size Δt :

$$Dist(t_i) = Dist(t_{i-1}) + V_{GS}(t_{i-1}) \cdot \Delta t. \quad (1)$$

The flight path angle γ is mainly a function of the constant (but variable) glidepath angle GPA corrected by the earth curvature represented by a simple distance-based approximation:

$$\gamma(t_i) = GPA + Dist(t_i) \cdot 1852/60. \quad (2)$$

Using the ground speed V_{GS} and the flight path angle γ the altitude is calculated:

$$Alt(t_i) = Alt(t_{i-1}) + V_{GS}(t_{i-1}) \cdot \Delta t \cdot \tan(\gamma(t_i)). \quad (3)$$

The calibrated airspeed is the final approach speed and is fixed during the whole segment. The final approach speed is a function of the stall speed V_{stall} and the headwind component of the wind $V_{headwind}$. If the headwind component is lower than 5 kts a safety threshold of 5 kts is added anyway:

$$V_{CAS}(t_i) = 1.23 \cdot V_{stall} + \max\{5kts; V_{headwind}\}. \quad (4)$$

The true airspeed V_{TAS} is the calibrated airspeed V_{CAS} corrected by the air density ρ at the current altitude:

$$V_{TAS}(t_i) = \frac{1}{\sqrt{\frac{\rho(Alt(t_i))}{\rho_0}}} \cdot V_{CAS}(t_i). \quad (5)$$

The ground speed V_{GS} is calculated using the true airspeed V_{TAS} considering the current flight path angle γ and the headwind component $V_{headwind}$:

$$V_{GS}(t_i) = V_{TAS}(t_i) \cdot \cos(\gamma(t_i)) - V_{headwind} \quad (6)$$

Please note that the calculation of the ground speed is a simplification. In reality the aircraft heads into the wind so that only the amount of the true airspeed heading into the direction of the ground track needs to be considered. However, as for the time being no three-dimensional wind information is used (only headwind component) and the calculation of the aircraft motion is limited to the longitudinal motion, this simplification is considered reasonable. This is especially true as typically the difference between track and heading of the aircraft is small, hence the error made through this simplification is small.

2.2.2 Flap deployment segment

Above the stabilisation altitude the approach is assumed to be flown with idle thrust. This means that depending on the actual glidepath angle the aircraft decelerates (or accelerates) during the final approach. Here, only approaches are considered where the aircraft still decelerates with idle thrust. In case that the aircraft would accelerate (e.g. because of a too steep glidepath angle) the use of spoilers would be required. At least for the simpler aerodynamic model of ANP the

additional drag due to the spoilers is not covered. For this reason, the use of spoilers is not considered here and the steepest glidepath angle is the one without acceleration without the use of spoilers.

The lowest speed to select the next flap configuration is the respective target speed for the current flap setting (e.g. CONF3 is selected when reaching the target speed of CONF2). Of course, the flaps can also be selected at any higher speed, as long as the speed is not above the maximum flap extension speed V_{FE} of the next flap configuration. For the backwards calculation this means that from timestep to timestep the speed must increase until reaching the target speed of the next lower flap configuration plus a specific additional speed ΔV . Through variation of ΔV the speed at which the flaps are deployed can be varied between the respective target speed (minimum) and the respective V_{FE} (maximum).

$$V_{target}(segment) = \begin{cases} 250 \text{ kts} & CONF0 \\ V_{greendot} + \Delta V & CONF1 \\ 1.23 \cdot V_{stall}(CONF1) + \Delta V & CONF2 \\ 1.23 \cdot V_{stall}(CONF3/4) + \Delta V & CONF3/4 \end{cases} \quad (7)$$

The target speed for clean configuration, hence the speed to select CONF1 is the so-called green dot speed. This is the speed with the best lift-to-drag-ratio and therefore it is aircraft dependent. Here, the green dot speed is used for the A320 family on the one hand and the A330 on the other as follows

$$V_{greendot} = \begin{cases} 2 \cdot \frac{m}{1000} + 107 & A319, A320, A321 \\ 0.6 \cdot \frac{m}{1000} + 80 & A330 \end{cases} \quad (8)$$

While the current calibrated airspeed $V_{CAS}(t_i)$ is lower than the respective target speed V_{target} the following aircraft parameter are calculated in the following way.

The aircraft mass is a pure summing of the idle fuel flow, which is kept constant here for reasons of simplification.

$$m(t_i) = m(t_{i-1}) + IdleFuelFlow \cdot \Delta t \quad (9)$$

The distance to the touchdown point on the runway is calculated identically as before by numerical integration of the ground speed V_{GS}

$$Dist(t_i) = Dist(t_{i-1}) + V_{GS}(t_{i-1}) \cdot \Delta t. \quad (10)$$

Below the glidepath intercept altitude the glidepath angle is calculated the same way as described before. Above the intercept altitude the flight path angle is zero.

$$\gamma(t_i) = \begin{cases} GPA + Dist(t_i) \cdot 1852/60 & Alt(t_{i-1}) < Alt_{Intercept} \\ 0 & Alt(t_{i-1}) \geq Alt_{Intercept} \end{cases} \quad (11)$$

The same applies for the calculation of the altitude, that is calculated based on the current flight path angle below the intercept altitude.

$$Alt(t_i) = \begin{cases} Alt(t_{i-1}) + V_{GS}(t_{i-1}) \cdot \Delta t \cdot \tan(\gamma(t_i)) & Alt(t_{i-1}) < Alt_{Intercept} \\ Alt_{Intercept} & Alt(t_{i-1}) \geq Alt_{Intercept} \end{cases} \quad (12)$$

The Mach number is calculated using the true airspeed of the previous timestep, as the current value of the true airspeed is still to be evaluated.

$$Ma(t_i) = \frac{V_{TAS}(t_{i-1})}{a(Alt(t_i))} \quad (13)$$

The lift coefficient is calculated with the current mass m , air density ρ , true airspeed V_{TAS} and the wing area S

$$C_L(t_i) = \frac{m(t_i) \cdot g}{\frac{\rho(Alt(t_i))}{2} \cdot V_{TAS}(t_{i-1})^2 \cdot S}. \quad (14)$$

Applying a trimmed polar model, the evaluation of the drag coefficient uses the actual lift coefficient, the Mach number and flap configuration. Applying the ANP model, only the lift coefficient and the respective flap configuration is required.

$$C_D(t_i) = f(C_L(t_i), Ma(t_i), CONFIG) \quad (15)$$

The current idle thrust per engine T_{eng_i} is provided by the respective aircraft performance model, too. The idle thrust only depends on the current altitude Alt and Mach number Ma

$$T_{eng_i}(t_i) = f(Alt(t_i), Ma(t_i)). \quad (16)$$

With the current thrust per engine T_{eng_i} , aircraft mass $m(t_i)$, drag coefficient C_D , lift coefficient C_L and flight path angle γ the current change of the true airspeed is evaluated. This value should always be negative, as the aircraft should decelerate during the final approach.

$$\frac{\partial V_{TAS}}{\partial t}(t_i) = \frac{T_{eng_i}(t_i) \cdot n_{eng}}{m(t_i) \cdot g} - \frac{C_D(t_i)}{C_L(t_i)} \cdot \cos(-\gamma(t_i)) - \sin(-\gamma(t_i)) \quad (17)$$

Once the current change of the true airspeed is known the current true airspeed V_{TAS} can be calculated by summing up the changes over time. Please note, that the change of true airspeed is subtracted here because of the backwards calculation (deceleration leads to a higher airspeed at the next timestep in backwards calculation direction).

$$V_{TAS}(t_i) = V_{TAS}(t_{i-1}) - \frac{\partial V_{TAS}}{\partial t}(t_i) \cdot \Delta t \quad (18)$$

The true airspeed is then transformed into calibrated airspeed V_{CAS}

$$V_{CAS}(t_i) = V_{TAS}(t_i) \cdot \sqrt{\frac{\rho}{\rho_0}}. \quad (19)$$

Finally, the current ground speed is calculated as the projection of the true airspeed on ground an by adding the headwind component. Please note again here the simplification by using the true airspeed instead of the projection of the true airspeed in track direction as described in section 2.2.1.

$$V_{GS}(t_i) = V_{TAS}(t_i) \cdot \cos(\gamma(t_i)) - V_{headwind} \quad (20)$$

During each cycle it is checked whether the calibrated airspeed would exceed the target speed if the flaps would be retracted at the respective time step given the configuration-specific

deployment time of the flaps and the average of the current and the predicted deceleration (please, remind the backwards calculation – “retraction” in the calculation is actually a deployment in reality). If this is the case the flaps are retracted linearly at each following time step so that the flap transition is finished when reaching the configuration-specific deployment time. By using the average value of the aircraft deceleration at the start and at the end of the flap transition the target speed is met pretty well when the flap transition is finished.

When the flaps are fully retracted, the respective flap segment is finished and the program switches to the next segment.

2.2.3 Segment without flap transition

If required, segments without a flap transition at the end of the calculation (or at the beginning in real flight) can be inserted in the sequence. This could be the case if e.g. deployment of the landing gear and the deflection of the flap configuration following the gear deployment should not be performed right after another. In this case the aircraft would continue to fly in real flight with the same flap configuration after lowering the landing gear.

The equations for this segment are identical with those depicted before in section 2.2.2 with the only difference, that the segment is not finished after reaching a target speed but after reaching a pre-defined distance in nautical miles and that no flap transition is calculated.

This way a specific distance in nautical miles can be added between lowering the landing gear and the deflection of the next flap configuration.

Deploying the landing gear earlier on the final approach is another means to increase the glideslope intercept speed similar to the additional flap deflection speed as described in section 2.2.2. However, it is desired to lower the landing gear as late as possible on the approach as the landing gear is a considerable source of noise. Also, the additional flap deflection speed is a much more effective means to increase the glideslope intercept speed. For, these reasons the segment without flap transition is not used here for the evaluation of the energy envelope.

2.2.4 Gear deployment segment

The gear deployment segment is generally calculated using the same equations as in section 2.2.2. However, the requirement for finishing the segment is the full retraction of the landing gear. Remember the backwards calculation for which reason the actual deployment of the gear is a retraction in the calculation.

2.2.5 Aerodynamics during gear and flap deployment

During gear and flap deployments the aerodynamics need to be changed continuously. Here, a linear transition of the aerodynamics is assumed. For all transition phases of the landing gear or flaps the aerodynamics are evaluated for the current flight state for both relevant flap positions (or gear, respectively). For example, if the flap transition from CONF2 to CONF3 is calculated (meaning, that in the backwards calculation the initial flap stet is CONF3 and the final flap state is CONF2) the $C_W(t_i)$ is calculated for both flap configurations and linearly interpolated for the current transition position (between 1 and 0).

2.3 Complete approach calculations

Through a variation of the flap extension speed from the target speed of the respective flap configuration to the respective V_{FE} of the next flap configuration the speed with which the glidepath is intercepted can be varied. Figure 1 shows these two extreme approaches for one example case with an intercept altitude of 3,000 ft and 3° glideslope angle.

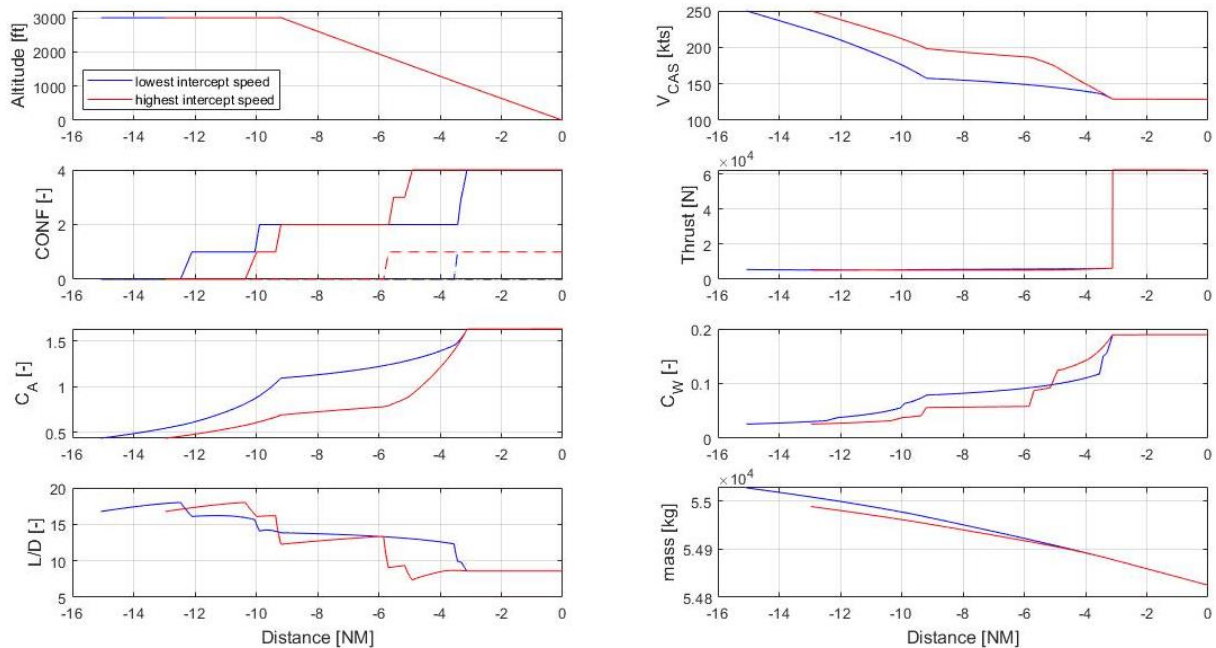


Figure 1: Exemplary approach with lowest and highest glidepath intercept speed (trimmed polar model).

One can observe in Figure 1 that in the red case the gear deployment and the configuration changes from Conf 2 to Conf Full is much earlier resulting in a much longer phase with high deceleration. Therefore, the intercept speed can be higher while the approach is still stable at 1,000 ft agl. In the other case the gear deployment and Configuration changes to Conf Full is

performed the latest resulting in a very long phase with only little deceleration. For this reason, the glidepath needs to be intercepted at a much lower speed in order to reach the final approach speed at the stabilisation height of 1,000 ft agl.

These two speeds form the speed boundaries for an optimal idle approach, hence for the speed envelope. In case that the intercept speed is higher the pilot inevitably needs to use spoilers for deceleration or otherwise the approach would not be stable at the stabilisation altitude. On the other hand, if the intercept speed is lower the lower boundary the aircraft would reach the final approach speed before reaching 1,000 ft agl., hence needs to increase thrust too early. Both cases increase noise and the too slow approach also leads to an unnecessary increase of fuel burn.

These boundaries of the speed envelope vary with glideslope angle, but also with the aircraft mass, the glidepath intercept altitude or wind. As there are too many influencing parameters the envelope can only be depicted for a set of parameters.

2.4 Graphical depiction of the envelope

Based on the calculations as described before the approach can be evaluated for different environmental conditions, aircraft mass and intercept altitude. If flaps and gear are always deployed at the latest possible moment (meaning when reaching the target speed of each configuration) the glidepath intercept speed is the lowest. If the flaps are always deployed right after reaching the maximum flap extension speed V_{FE} of the next configuration the intercept speed is the highest. These two values form the boundaries of the speed envelope. In between these two speed boundaries the approach can be performed in idle thrust. Figure 2 shows an example of the speed envelope for an A320 with a gross weight of 55 tons, an intercept altitude of 3,000 ft and no wind.

Figure 2 shows the lines of the minimum and maximum intercept speed as a function of the glideslope angle. In between these speeds an optimal approach can be performed, which means that the approach can be flown with idle thrust until reaching the final approach speed at the stabilisation height. The higher the intercept speed (within the boundaries of the envelope) the earlier gear and flaps need to be deployed in order to reach the final approach speed at the stabilisation height.

However, this does not mean that a flight outside the envelope is not possible. Intercepting the glidepath with a higher speed than the upper speed boundary inevitably requires the use of spoilers in order to decelerate the aircraft. This is indeed flyable, but as it increases the noise it is undesired and should be avoided. On the other side, intercepting with a lower speed leads to a too early reaching of the final approach speed, hence a too early thrust increase. This is of course flyable as well, but leads to a noise and fuel burn increase and should therefore be avoided as well.

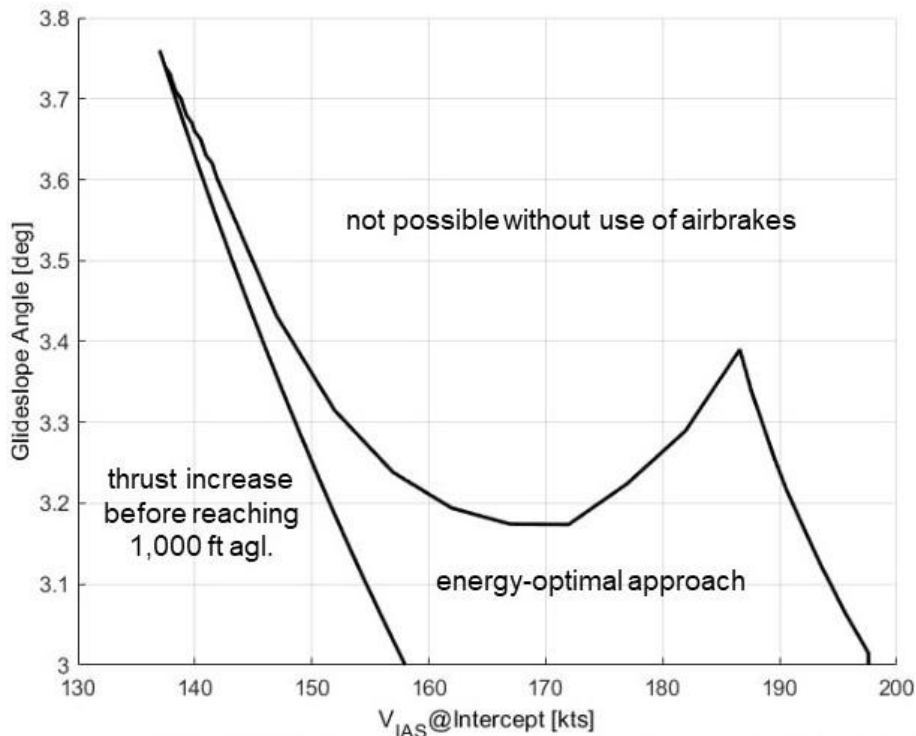


Figure 2: Exemplary depiction of the speed envelope (trimmed polar model).

As can be seen in Figure 2 the two boundaries cross each other at a specific glideslope angle. At any steeper glideslope angle the use of spoiler for deceleration is unavoidable or the aircraft needs to be fully configured before reaching the glidepath intercept. Both consequences are undesired and therefore the maximum glideslope angle depicted by the speed envelope is indeed not a flight physical limitation but should not be exceeded for optimal low noise approaches.

If the glidepath intercept speed lies within the speed envelope the aircraft needs to be configured accordingly, in order to reach the final approach speed at stabilisation height. Figure 3 shows the intercept speed-dependent altitudes at which the landing gear and the final flap configurations need to be deployed. Here, the limits of the y-axis are the boundaries of the speed envelope for an exemplary glideslope angle of 3° as shown in Figure 2.

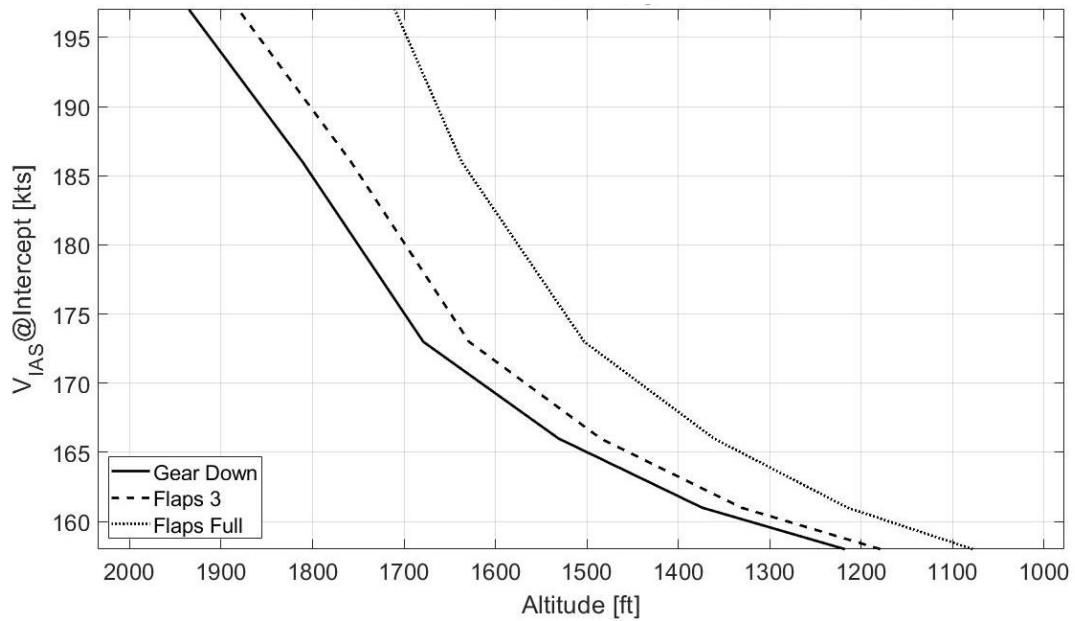


Figure 3: Exemplary depiction of the configuration altitudes (trimmed polar model).

It is obvious that the aircraft needs to be configured earlier (meaning at higher altitudes) the faster the glidepath is intercepted.

Both the shape of the speed boundary as well as the shape of the intercept-speed-dependent configuration altitudes may vary with the aerodynamics and thrust models used for the calculation. The examples depicted here were generated using a trimmed polar models of the A320. This issue will be addressed in section 3.2

3 Verification

Validation of the approach calculation can only be performed by comparison to real flight data. As the most important parameter for the generation of the energy envelope is the intercept speed, the calculated speed profile along the glidepath is crucial to be accurate. If the speed profile along the glidepath is accurate, the correctness of the intercept speed is verified. Also, the used aircraft performance model is crucial, as it influences the aircraft's deceleration ability, therefore the speed profile along the glidepath. The verification of the correctness of the intercept speed under given circumstances, such as aircraft mass, wind etc., is described in the following.

3.1 Comparison to real flight data

In order to compare the calculated approach with real flight data, the backwards calculation as described in section 2.2 needs to be slightly adopted.

First, the wind needs to be covered accurately in terms of speed and direction. Therefore, wind information from the respective flight data are fed into the approach calculation as a function of the aircraft's altitude.

Secondly, the aircraft's vertical flight path needs to be adopted in the calculation. Under real flight conditions aircraft never fly exactly on the glideslope, for which reason the flight path angle slightly varies during the final approach. These slight changes in the flight path angle, however, lead to a change in the deceleration characteristics. For this reason, the speed profile can never be matched in case that for the calculation a constant flight path angle (e.g. -3°) is assumed, whilst in reality the aircraft flew with a slightly varying flight path angle. In order not to compare apples and oranges, the actual flight path angle from the flight data is used in the backwards calculation as a function of the aircraft's altitude. This way, the simulated flight path follows the real flight path accurately, leading to a much more precise speed profile.

Thirdly, the aircraft configuration must fit. For this reason, flaps/slats and landing gear are deployed in the simulation at the exactly same altitude as in the flight data.

Also, the final approach speed and the actual stabilisation height needs to be adapted in order to match the flight data.

This way, the calculated approach can be compared with real flight data, showing the accuracy of the calculated speed profile, hence intercept speed.

Flight data for comparison are available for the A320 and B737-800. For the A320 flight data with glideslope angles of 3° and 3.2° are available, for the B737 only 3° approaches are available. Flight data with steeper glidepath angles are not available. However, the general correctness of the method of the approach calculation can be verified also with the available flight data.

3.1.1 A320

For the verification against A320 flight data a trimmed polar model is used as it is considered to provide more accurate results as the ANP model. Figure 4 and Figure 5 exemplarily show two different approaches of A320 aircraft with a glideslope angle of 3° . The upper row of subplots shows the inputs as they were taken from the flight data, namely the flap and gear deployment as well as wind speed and direction. The lower row of subplots shows the altitude and - most importantly - true and ground speed, as well as the aircraft mass.

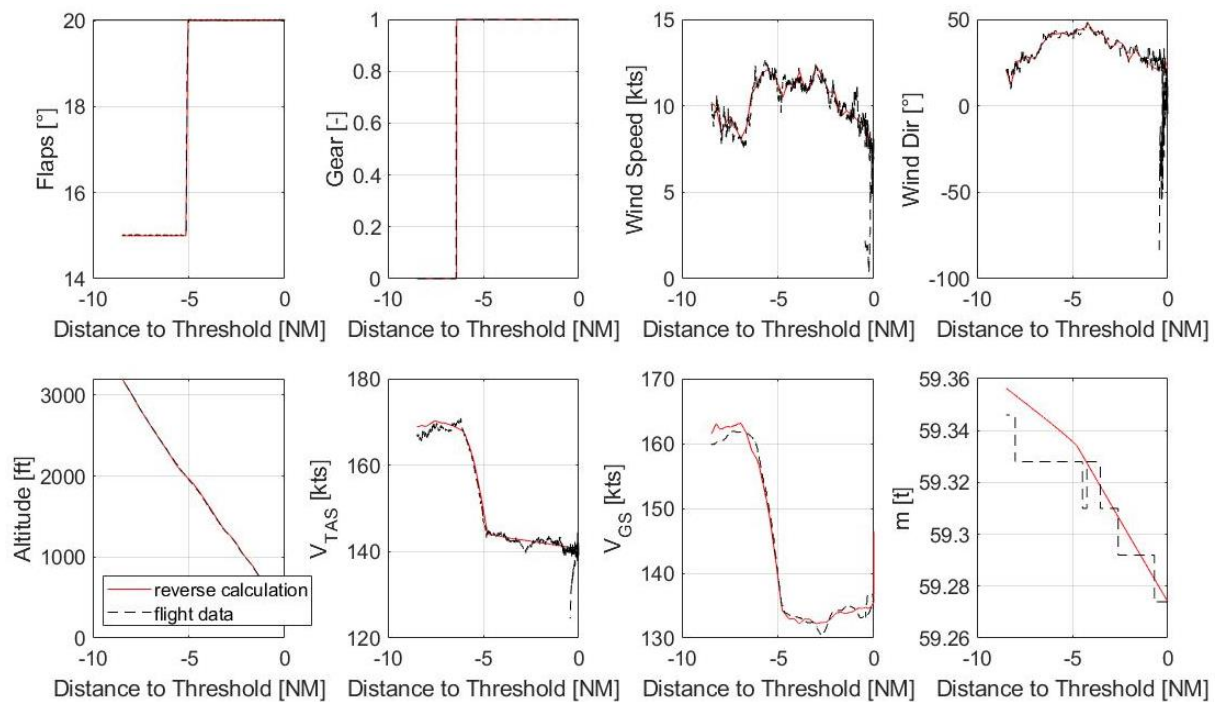


Figure 4: Fit of backwards simulation and flight data of A320 with trimmed polar model (3° glideslope angle).

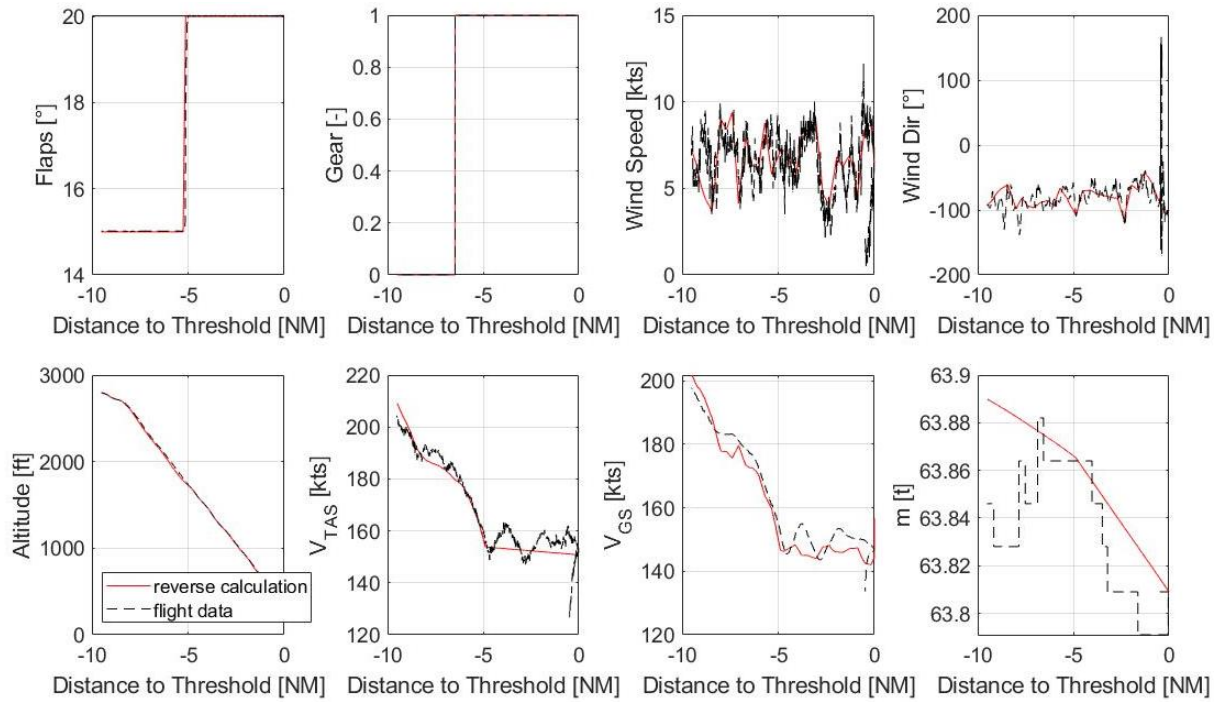


Figure 5: Fit of backwards simulation and flight data of A320 with trimmed polar model (3° glideslope angle).

One can observe in Figure 4 and Figure 5 that the profile of both true and ground speed fits well to the real flight data. The calculated intercept speed fits well to the one of the real flights.

In addition, Figure 6 shows an approach with a glideslope angle of 3.2° . Also, in this case the calculated speed profile matches the one from the real flight acceptably well.

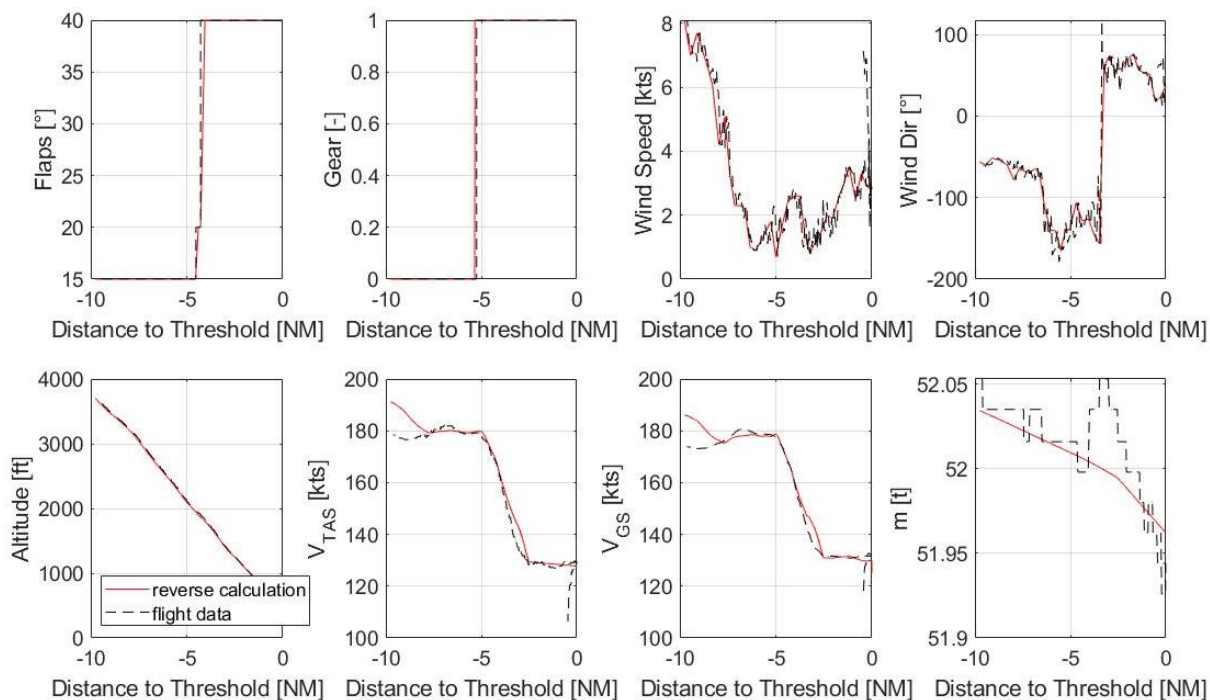


Figure 6: Fit of backwards simulation and flight data of A320 with trimmed polar model (3.2° glideslope angle).

For reasons of completeness, the same approach as shown in Figure 6 is calculated using the ANP model. The resulting profile of the true airspeed is depicted in Figure 7. As can be seen in the figure the calculated profiles of the true airspeed is of comparable accuracy for both models in this case.

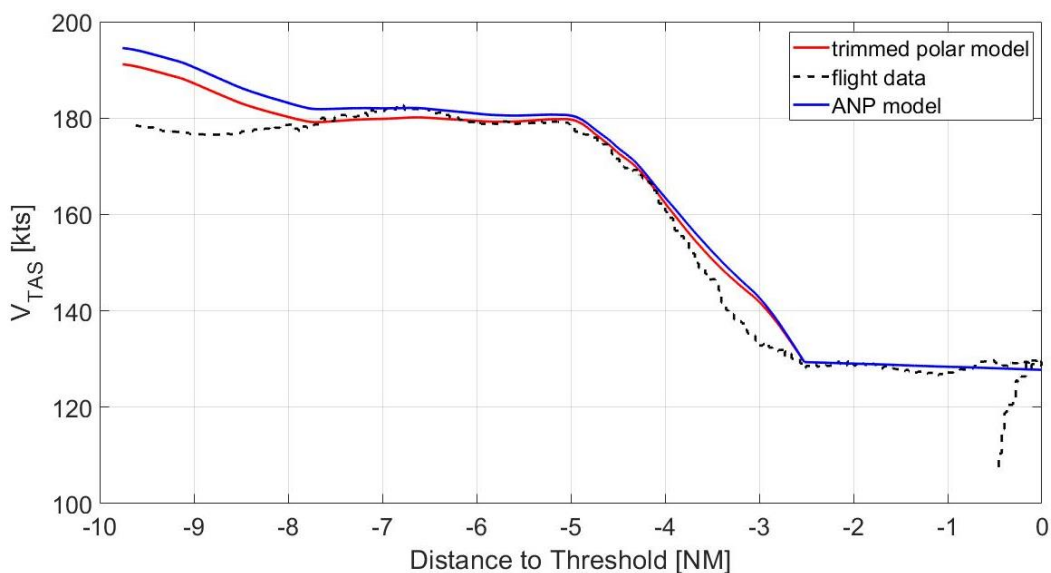


Figure 7: Comparison of backwards simulation and flight data of A320 with trimmed polar model and ANP model (3.2° glideslope angle).

The comparison with real flight data shows that the used method of the backwards calculation is able to deliver speed profiles of acceptable accuracy for the A320 with glideslope angles of 3° and 3.2° using a trimmed polar model. As a trimmed polar model uses nonlinear aerodynamics, it can be expected that the results for steeper glideslope angles are of comparable accuracy. Using the ANP model also delivers sufficiently accurate results for glideslope angles of 3° and 3.2° . For steeper glideslope angles, however, it is questionable how accurate the results are, because of the linear aerodynamics that are incorporated in ANP. Unfortunately, no flight data for steeper glideslope angles are available.

3.1.2 B737-800

For the B737-800 flight data are available but no trimmed polar model. For this reason, the ANP model was used for the comparison of calculated approaches with real ones. The experience with the A320 showed that the ANP model is able to deliver results of acceptable accuracy. For the B737-800, however, the comparison of calculated approaches and real flight data revealed a substantial mismatch for the deceleration ability in with flaps at 5° . Figure 8 to Figure 10 show comparisons between computed and real approaches with the original ANP model.

The reader should be aware that in the data of the ANP model no distinction between flap and gear deployment is made. For this reason, gear and flaps cannot be deployed independently from each other (such as for the A320, where parameters exist for specific flaps settings with and without landing gear). Here, with the B737-800 flap and gear extension is connected, so that it does not make sense to show a separate graph for the landing gear.

One can observe in Figure 8 to Figure 10 that the deceleration for any flap deflection greater than 5° is acceptable. For the 5° flap segment, however, the deceleration is obviously overrated in the calculations.

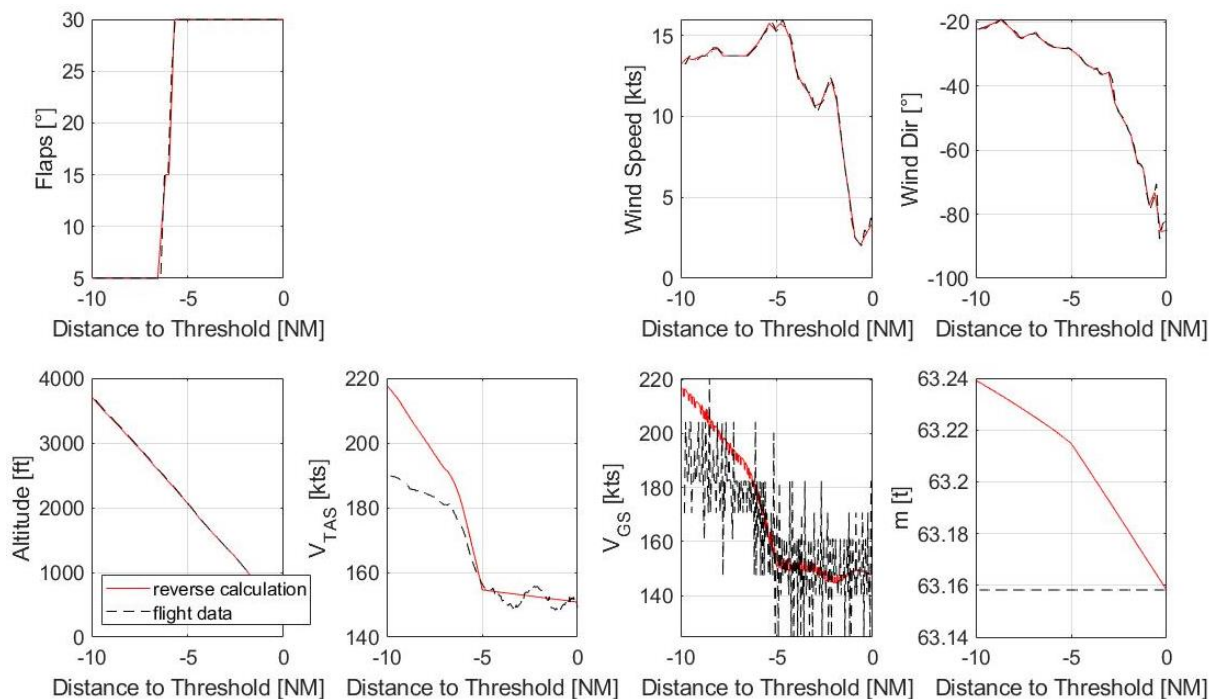


Figure 8: Fit of backwards simulation and flight data of B737-800 with original ANP model (3° glideslope angle).

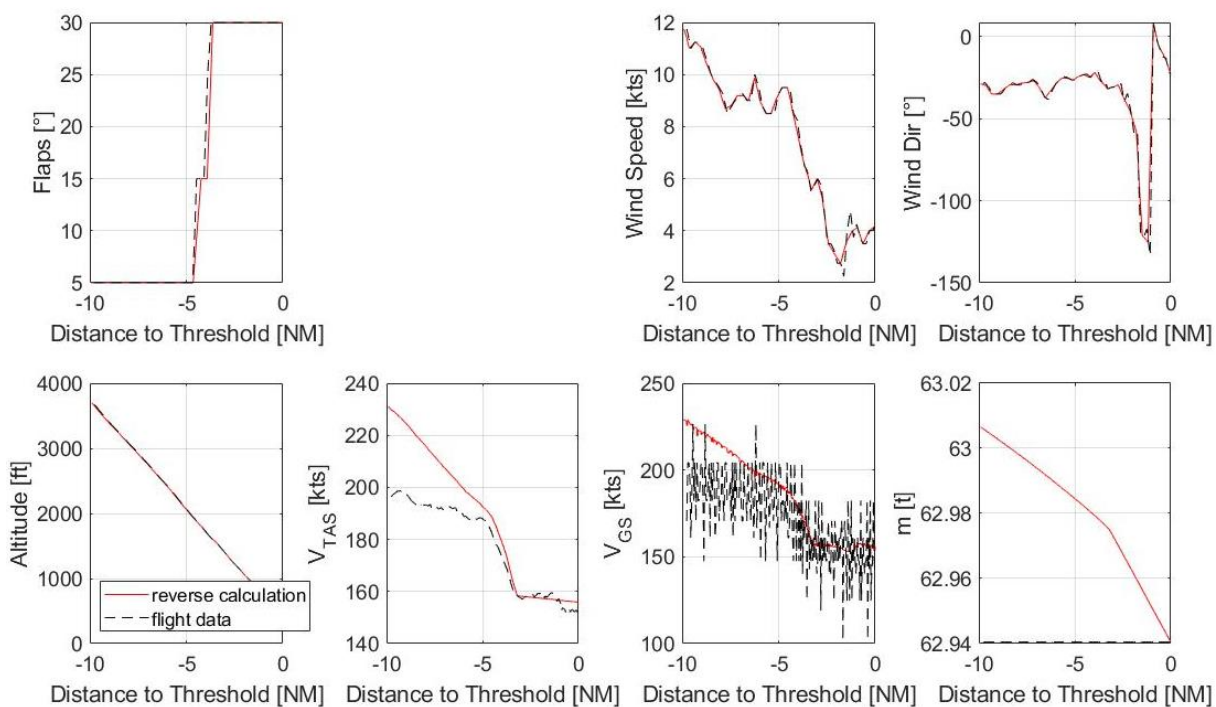


Figure 9: Fit of backwards simulation and flight data of B737-800 with original ANP model (3° glideslope angle).

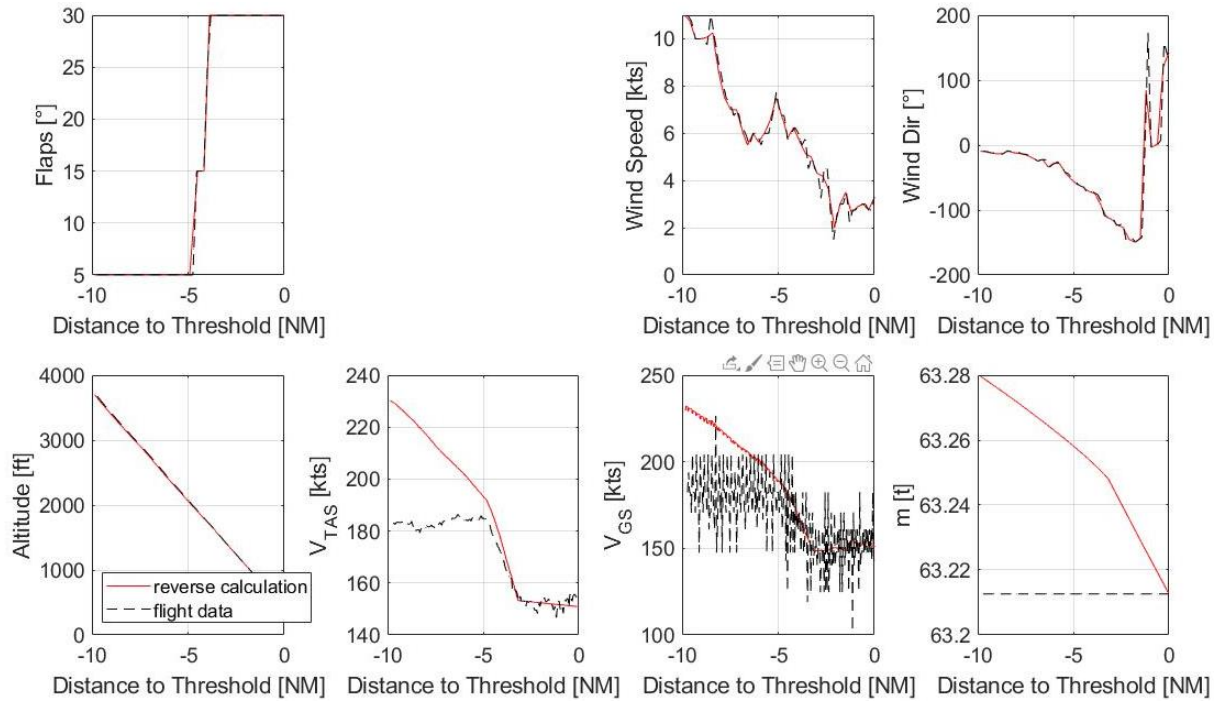


Figure 10: Fit of backwards simulation and flight data of B737-800 with original ANP model (3° glideslope angle).

In order to fix this obviously wrong lift-to-drag-ratio for the 5° flap deflection given by the original ANP model, this parameter was adapted in a way that the speed profiles fit better to the flight data. Figure 11 to Figure 13 show the same approaches as Figure 8 to Figure 10 but with the adapted ANP model.

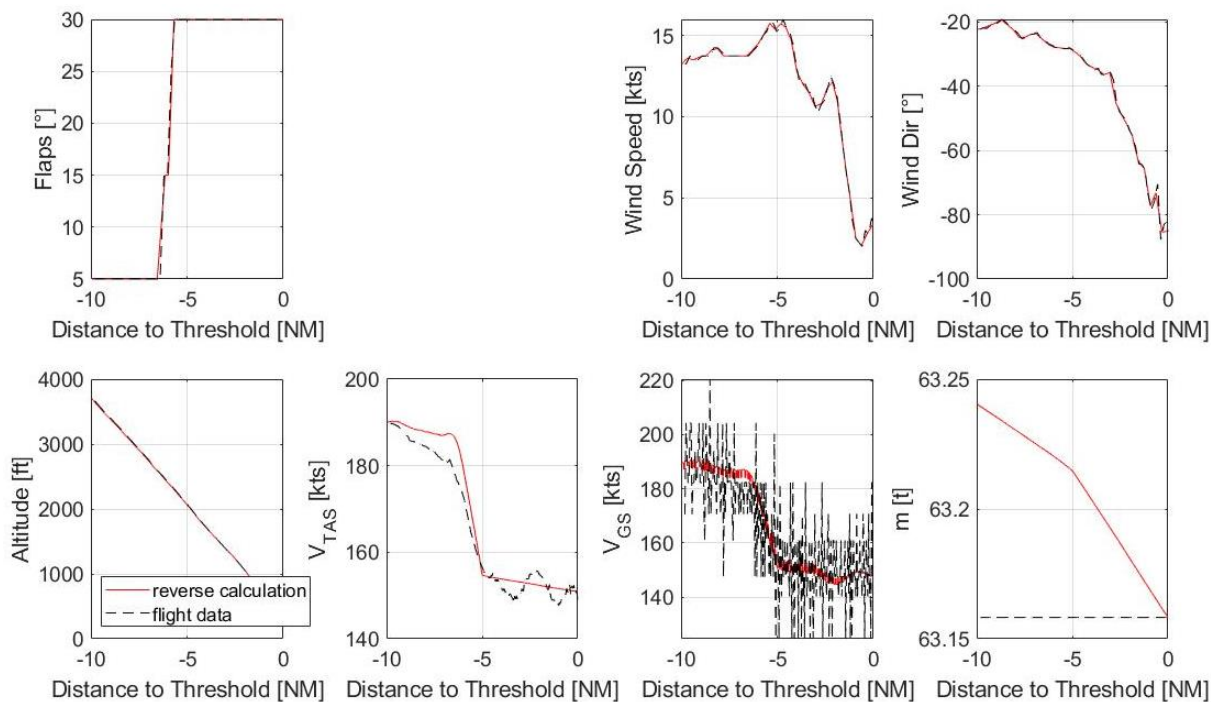


Figure 11: Fit of backwards simulation and flight data of B737-800 with adapted ANP model (3° glideslope angle) – same flight as in Figure 8.

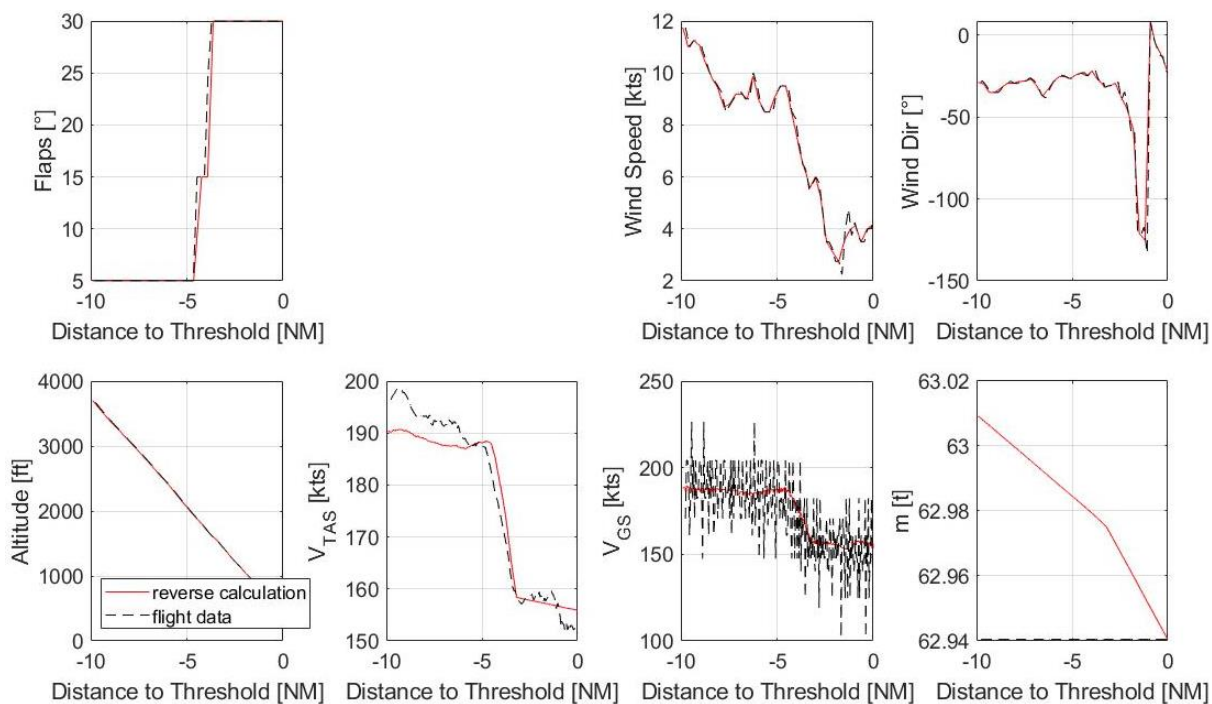


Figure 12: Fit of backwards simulation and flight data of B737-800 with adapted ANP model (3° glideslope angle) – same flight as in Figure 9.

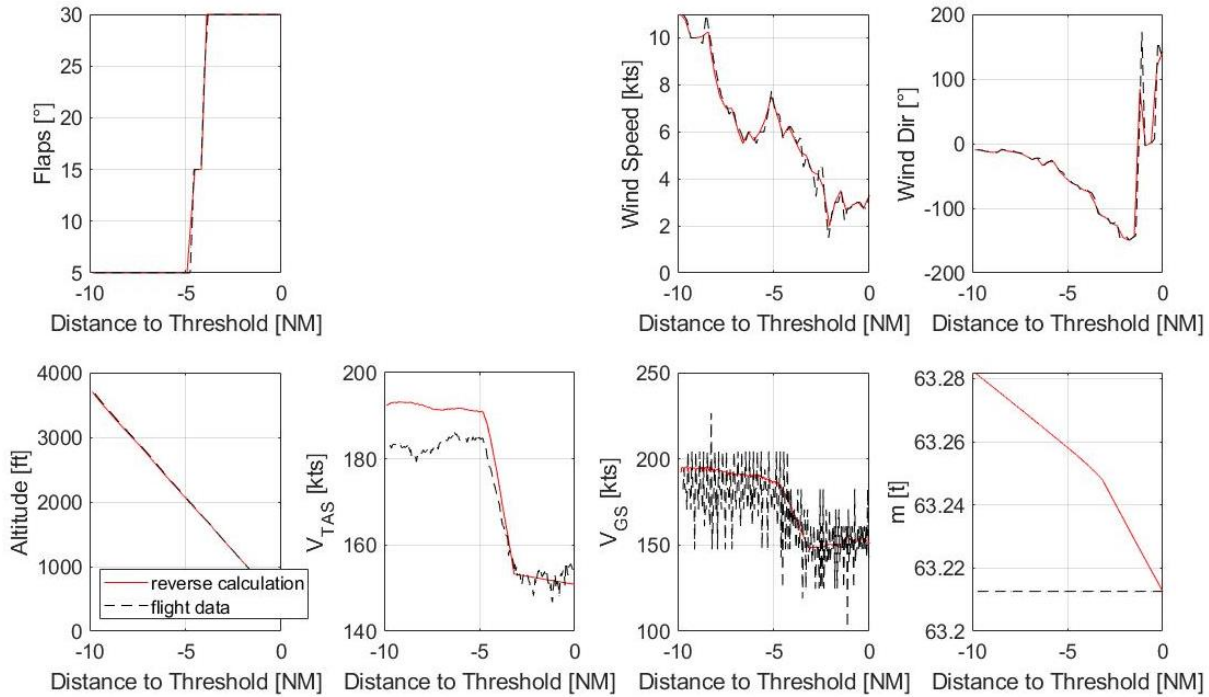


Figure 13: Fit of backwards simulation and flight data of B737-800 with adapted ANP model (3° glideslope angle) – same flight as in Figure 10.

Figure 11 to Figure 13 show that with the adaptation of the lift-to-drag-ratio of the 5° flap deflection the speed profiles of all three approaches matches the flight data much better. The accuracy, however, is not as good as shown for the A320 with ANP model (see previous section 3.1.1). Through the adaptation of the ANP model as outlined here, it should be shown that with an appropriate model the used method of the backwards calculation is able to deliver results of acceptable reliability.

3.2 Variation of aircraft performance models

As shown before the comparison of calculation and real flight data for single approaches revealed a sufficient agreement for both models used here, a trimmed polar model and the ANP model. In order to further analyse the influence of the chosen aircraft performance model on the energy envelope Figure 14 shows the direct comparison of calculation results with a trimmed polar model and the ANP model for the A320.

The left column of plots shows an approach with flap settings always at the lowest speed possible (when reaching the respective target speed of each configuration). This results in the lowest intercept speed. The right column of plots shows an approach an approach with flap settings always at the highest speed possible (right after reaching the respective VFE of the following configuration). This results in the highest intercept speed. Both cases are simulated with both aircraft performance models (trimmed polar model and ANP). The approach conditions in terms of wind, aircraft mass, etc. are the same for each approach.

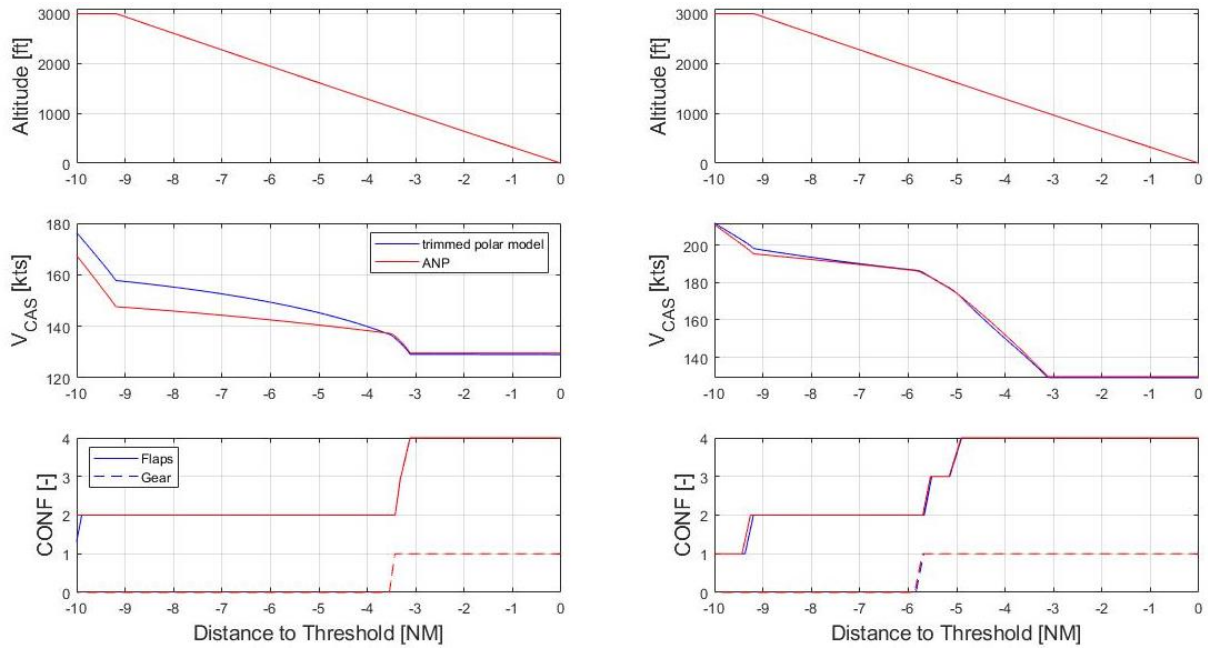


Figure 14: Comparison of trimmed polar model and ANP for A320 with 55 t and no wind (left: highest speed intercept; right: lowest speed intercept).

Figure 14 shows that for higher intercept speeds (right side) both models agree quite well. For low intercept speeds (left side), however, the speed profile is different, resulting in a difference in the intercept speed of about 10 kts. These results only apply for a glideslope angle of 3° . For steeper glideslope angles the differences between both aircraft performance models can be expected to increase, as the ANP model applies a linear approximation of the drag characteristics. The further away from the flight point originally intended by ANP the model is applied the greater will be the error made.

Figure 15 depicts the full energy envelope evaluated with both models. One can observe the same characteristic as explained above by means of Figure 14. For the glideslope angle of 3° the envelope boundaries of both models are relatively comparable for higher speeds, but for lower speeds the envelope boundaries differ by about 10 kts. Hence, for higher airspeeds ANP represents a trimmed polar model relatively well. Also, the maximum glideslope angle achievable with idle thrust at higher speeds (the right peak of the envelope) is met relatively well. However, the nonlinear shape of the envelope's upper boundary and the high peak at low intercept speeds are totally different.

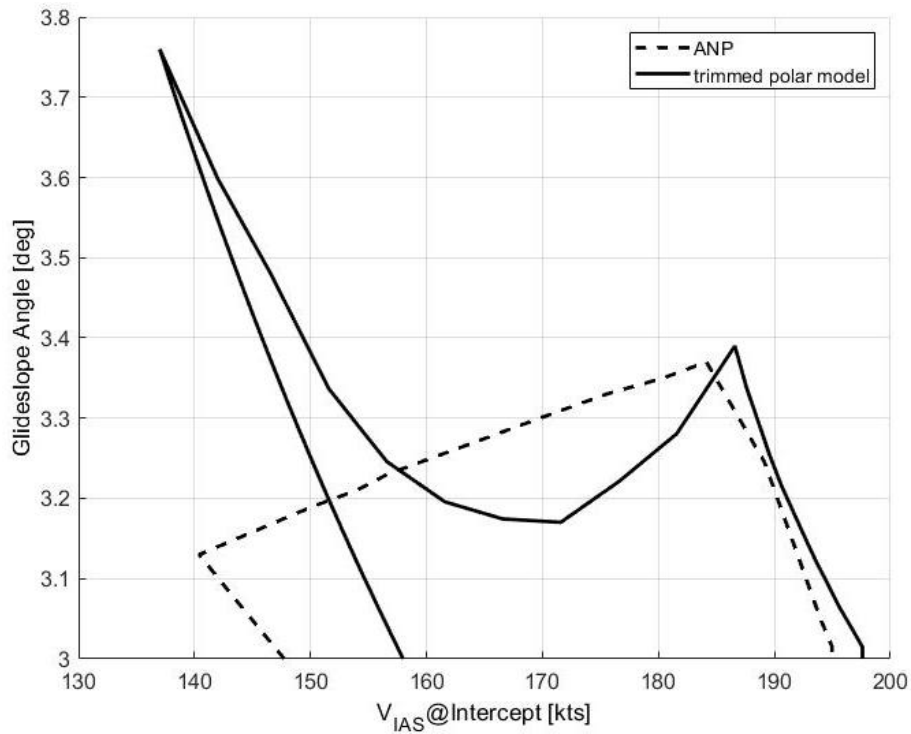


Figure 15: Influence of the used model on the speed envelope (A320, aircraft mass 55 t, intercept altitude 3,000 ft, no wind).

Concluding, one can state that due to the fact that ANP applies a linear approximation model for the aerodynamics the accuracy is worse outside of today's typical flight regime, e.g. at steeper approaches. For today's standard approaches (3° glideslope angle) the ANP model is considered a good alternative but with decreasing accuracy for steeper glideslope angles. If feasible a trimmed polar model with nonlinear aerodynamics should be used.

4 Results for different aircraft types

The shape of the energy envelope is influenced by any factor that influences the flight performance, hence the ability of an aircraft to fly energy-efficiently. Those are e.g., the aircraft mass and the altitude at which the glideslope is intercepted, but also wind.

In the following energy envelopes are shown for narrow-body transport aircraft, represented by the Airbus A320 family, and wide-body aircraft, represented by the Boeing B787-9. Especially the A320 family provides an interesting opportunity for comparison of the energy envelopes and the different feasibility to fly approaches with increased glideslope angles in an energy-efficient manner. Based on the A320 as example aircraft a discussion on the variation of fuel consumption and noise immissions within the energy envelope is given.

4.1 Airbus A319

For the Airbus A319, a trimmed polar model is used for evaluation of aerodynamics and idle thrust.

As mentioned before, the aircraft mass is one of the major influencing parameters. Figure 16 shows different energy envelopes for the A319 with different aircraft masses. The aircraft mass denoted here is always the mass that the aircraft has at touchdown.

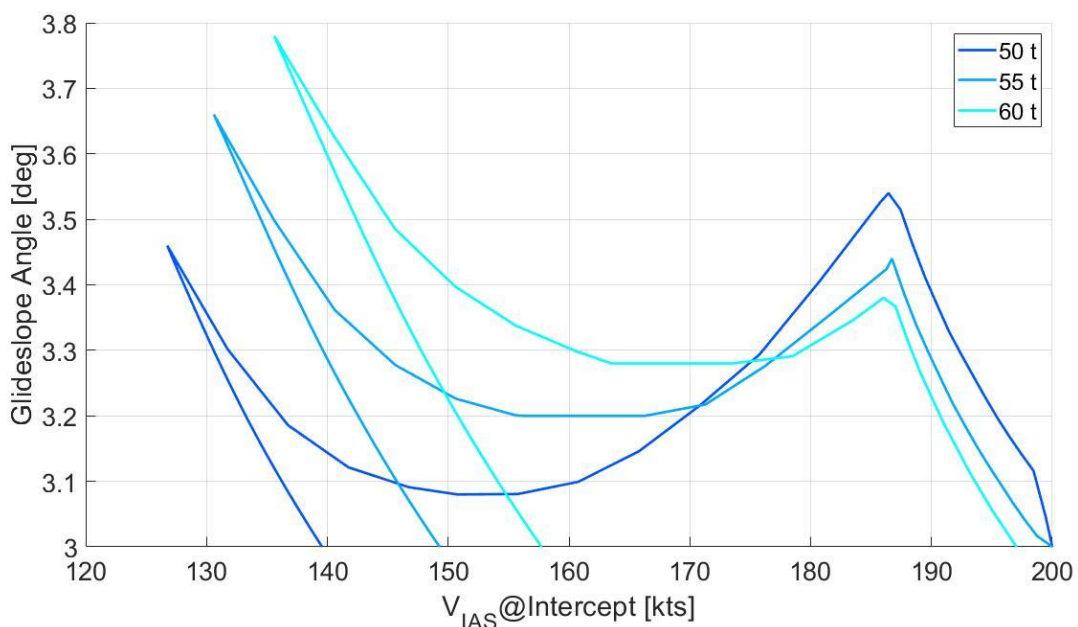


Figure 16: Influence of aircraft mass on speed envelope for A319 (intercept altitude 3,000 ft, no wind)

One can clearly see how big the influence of the aircraft mass is on the shape of the energy envelope and on the ability of the aircraft to fly energy-efficient approaches given a specific

glideslope angle. Interestingly, the influence of the aircraft mass on the two peaks of the maximum glideslope angle is different. While the left peak at lower intercept speeds increases with increasing aircraft mass, the right peak at higher intercept speeds decreases with increasing aircraft mass. This is an interesting outcome, as it does not support any of the two general opinions, that heavier aircraft can either fly steeper or not – this depends on the intercept speeds, at least in case that the approach is to be performed in an energy-efficient manner. For an intercept speed of e.g., 180 kts the lightest aircraft can fly the steepest glideslope angle, whereas for an intercept speed of e.g., 160 kts the heaviest aircraft can fly the steepest approach.

Another influencing parameter is the glideslope intercept altitude. At the first glimpse, this parameter might not be very obvious to be an influencing parameter, but a change of the intercept altitude changes the shape of the energy envelope and the ability to fly energy-efficient approaches significantly, as can be seen in Figure 17. The major effect from this is the change of air density with increasing intercept altitude, which influences the deceleration rate of the aircraft. The other effect is that with increasing intercept altitude, the distance and flight time between intercept and touchdown is increased as well, resulting in higher required intercept speeds to prevent to reach the final approach speed too early. For this reason, the energy envelope is shifted towards higher intercept speeds with increasing intercept altitude, but it also shrinks in size.

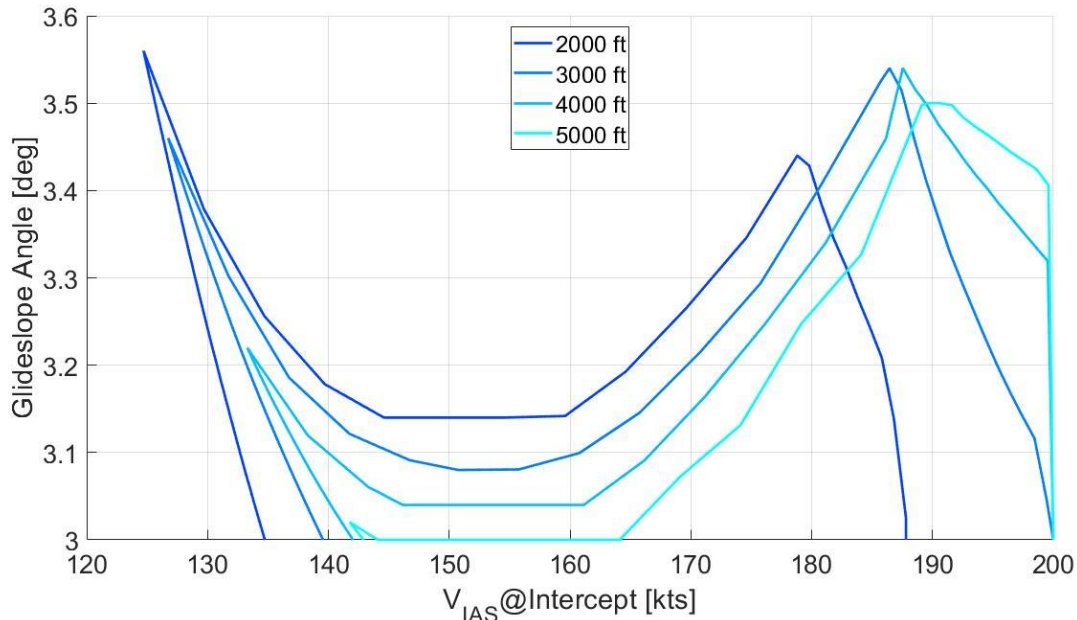


Figure 17: Influence of intercept altitude on speed envelope for A319 (aircraft mass 55 t, no wind)

Figure 17 shows that an increasing glideslope intercept altitude leads to a decreasing maximum glidepath angle over a wide range of intercept speeds. Only for high intercept speeds the maximum possible glideslope angle is nearly unchanged, although the right peak of the envelope moves towards higher intercept speeds. However, for an intercept speed of e.g., 180 kts the

maximum possible glideslope angle decreases from about 3.42° to about 3.26° if the intercept altitude is increased from 2,000 ft to 5,000 ft.

This means that if it is intended to increase the glideslope angle, the respective intercept altitude should be rather lower than higher than before. Otherwise, the risk occurs that pilots are not able to fly the approaches in an energy-efficient way and that the intended noise reduction from the glideslope angle increase is at least partly reversed by the use of airbrakes in order to reduce the aircraft's speed.

The third and maybe strongest parameter that influences the shape of the energy envelope is the wind. Headwind or tailwind change the ability of the aircraft to decelerate during final approach, hence the wind has a significant influence on the aircraft's ability to fly steeper approaches still in an energy-efficient manner. Figure 18 depicts the energy envelopes for different wind speeds. In this case the wind is always parallel to the flight direction, meaning without any crosswind component. Negative wind speeds are tailwinds, positive wind speeds are headwinds. Please note, that for reasons of simplification, the wind is constant here during the whole approach. This is, of course, not true in reality. However, the effects due to headwind or tailwind as shown here are generally the same, even if the wind speed changes during the approach.

The effect due to wind can be explained by two different reasons. First, as during the final approach the aircraft has to follow the glideslope, it flies with a given flight path angle. Therefore, the wind changes the aerodynamic flight path angle, meaning the flight path angle flown through the moving air. This angle is relevant for the deceleration. With prevailing tailwind, the aerodynamic flight path angle is steeper, resulting in a lower deceleration. With headwind, the aerodynamic flight path angle is shallower, resulting in an increased deceleration, or an improved ability of the aircraft to fly steeper glideslope angles. The second effect is the change of the ground speed due to the wind. As the distance between glideslope intercept and the threshold is constant (for the same glideslope angle), the remaining flight time is changed by the change of the ground speed. This leads to a lower intercept speed in case of tailwind (larger ground speed) even with the same deceleration rate – and vice versa.

Figure 18 clearly shows the above-mentioned effects. It is obvious how much the wind increases or decreases the ability to fly steeper approaches. With a constant tailwind of 20 kts, the energy envelope shrinks so much that only a narrow region of intercept speeds between 170 kts and 190 kts and between 140 kts and 150 kts is possible for the standard 3° approach. Already for a glideslope angle of 3.2° there is almost no possibility to fly energy-efficiently with a constant tailwind of 20 kts. On the other hand, Figure 18 shows how effectively headwind increases the possibility to fly steeper approaches. With a constant headwind of 20 kts, a glideslope angle of 3.8° is possible in an energy-efficient way with an intercept speed of about 187 kts. With a constant headwind of 40 kts, a maximum glideslope angle of even 4.1° is possible for still energy-efficient flights. However, Figure 18 also shows that with a constant headwind of 40 kts it is not possible to fly energy-efficiently at all with a glideslope angle lower than 3.3° , at least not if the glideslope is intercepted with flaps in Config 2. In this case the deceleration rate with idle thrust is too large, so that the aircraft always reaches its final approach speed before reaching 1,000 ft. In some of these cases it is possible to intercept the glideslope with flaps in Config 1, allowing to

fly the approach energy-efficiently. This gives another energy envelope for glideslope intercepts with flaps in Config 1.

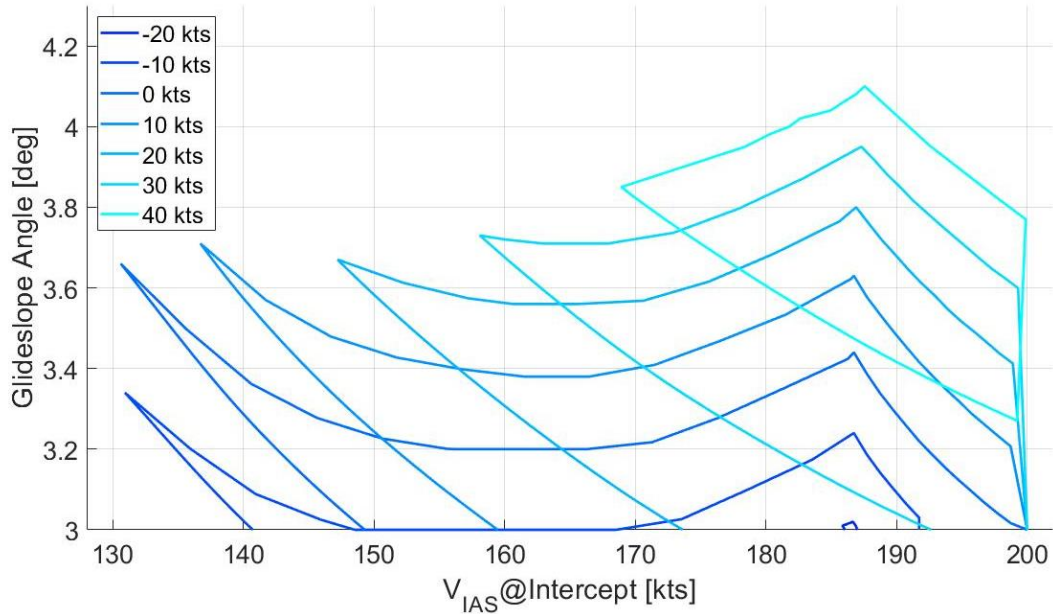


Figure 18: Influence of headwind component on speed envelope for A319 (aircraft mass 55 t, intercept altitude 3,000 ft) – intercept with Config2 only.

Figure 19 outlines the two energy envelopes for glideslope intercepts with flaps in Config 1 (dashed envelope) and Config 2 (solid envelope) for two cases with strong headwinds (30 kts and 40 kts). One can observe the envelopes for the Config 1 intercepts below the ones for Config 2 intercepts. However, the gap between the envelopes for Config 1 and Config 2 is also obvious, and this gap even increases with increasing headwind.

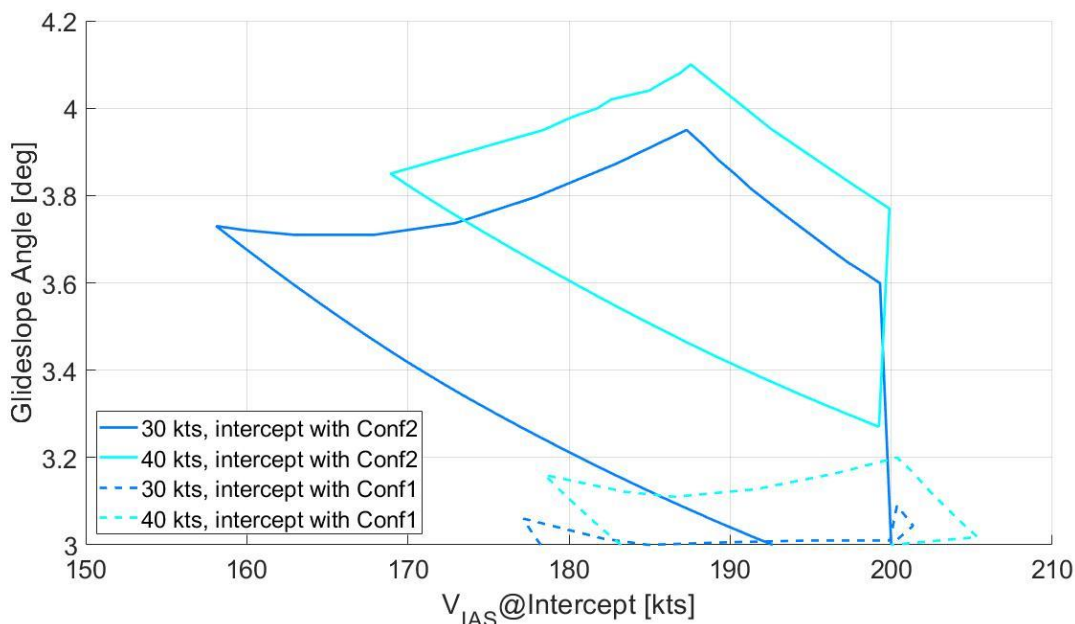


Figure 19: Influence of headwind component on speed envelope for A319 (aircraft mass 55 t, intercept altitude 3,000 ft) – intercept with Config1 and Config2.

One example shall illustrate the difficulties, which can be observed in Figure 19. For the extreme case of 40 kts headwind and given an intercept speed of 190 kts, a 3° glideslope angle is possible in an energy-efficient way with a glideslope intercept with flaps in Config 1. With increasing glideslope angle and still an intercept speed of 190 kts, the ability of the aircraft to decelerate in the Config 1 segment of the final approach is degraded. At a glideslope angle of a bit more than 3.1°, the boundary is reached where the aircraft does not decelerate anymore in Config 1. From this point on, with increasing glideslope angle, the aircraft requires speed brakes in order not to accelerate. However, if the glideslope was intercepted here with flaps in Config 2, the deceleration rate of the aircraft was too large, resulting in reaching the final approach speed too early. For this reason, no energy-efficient flight is possible here. Only with a glideslope angle of more than 3.4° (in the exemplary case of an intercept speed of 190 kts) it is again possible to fly energy-efficiently but with a glideslope intercept in Config 2. This is possible up to a glideslope angle of slightly more than 4°, above which the aircraft needs to use air brakes in any case.

For the extreme case of a constant headwind of 40 kts, Figure 19 also shows that no energy-efficient solution exists, for example, for a glideslope angle of between 3.3° and 3.4° (given this aircraft mass and intercept altitude).

Figure 18 and Figure 19 reveal the great influence that wind has on the possibility to fly approaches in an energy-efficient manner. It also shows, that for some extreme cases no energy-efficient solution might exist. Of course, applying a constant wind along the glidepath is not realistic. However, it was intended to show the most influencing effects on energy-efficient flight in a simplified way. In reality, with changing wind along the glide, it is even harder or maybe nearly impossible for pilots to always fly energy-efficiently without any kind of assistance system. The

outcome of the presented work even more justifies the introduction of any kind of energy assistance system in order to enable energy-efficient flight with increased glideslope angles.

4.2 Airbus A320

For the Airbus A320, a trimmed polar model is used for evaluation of aerodynamics and idle thrust.

The general shape and the influences of the parameters aircraft mass, intercept altitude and wind on the shape of the energy envelope is the same as for the A319. For a detailed description and explanation of the figures the reader should refer to section 4.1.

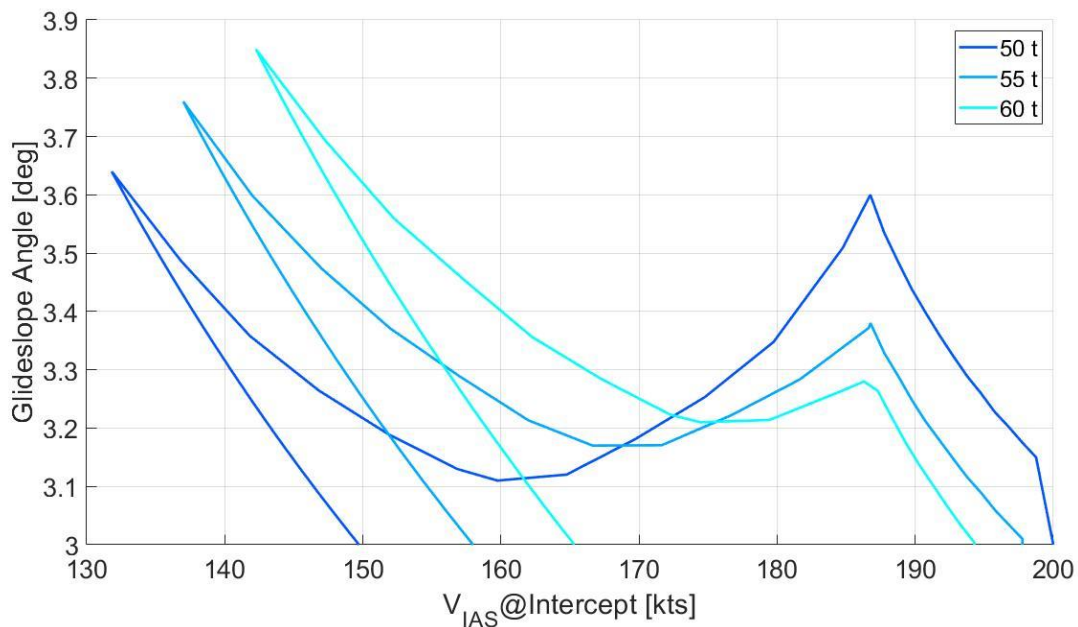


Figure 20: Influence of the aircraft mass on the speed envelope for A320 (intercept altitude 3,000 ft, no wind).

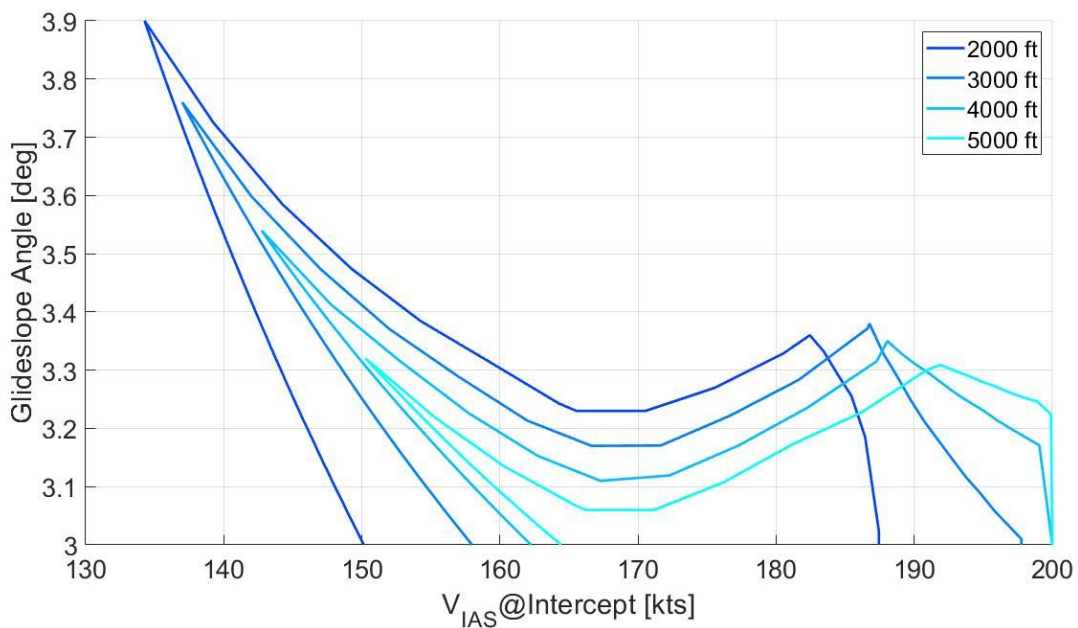


Figure 21: Influence of the intercept altitude on the speed envelope for A320 (aircraft mass 55 t, no wind).

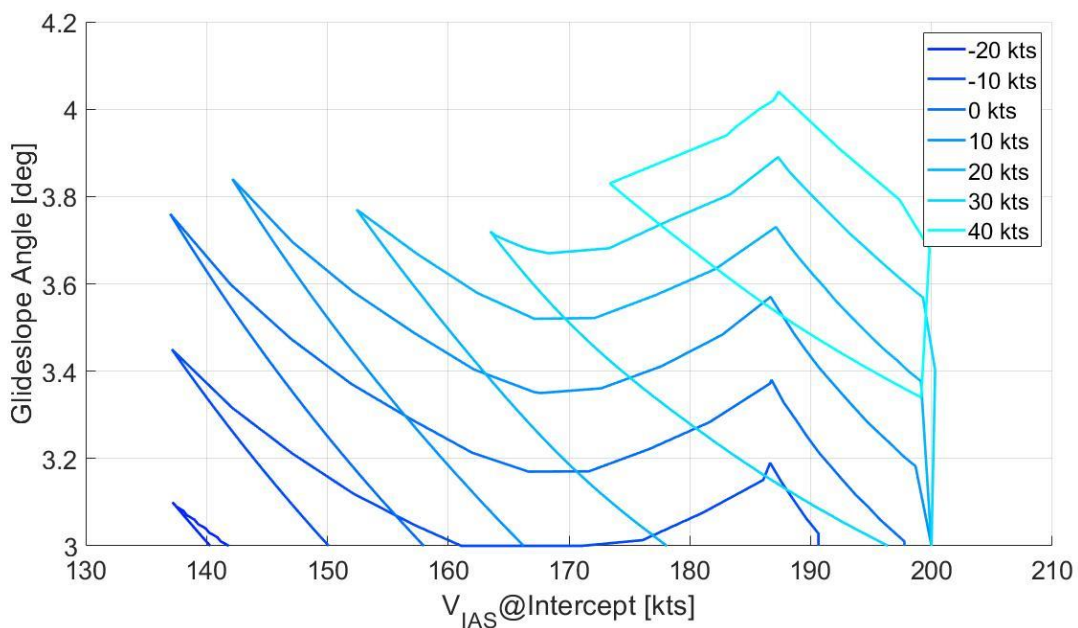


Figure 22: Influence of the wind on the speed envelope for A320 (aircraft mass 55 t, intercept altitude 3,000 ft) – intercept with Config2 only.

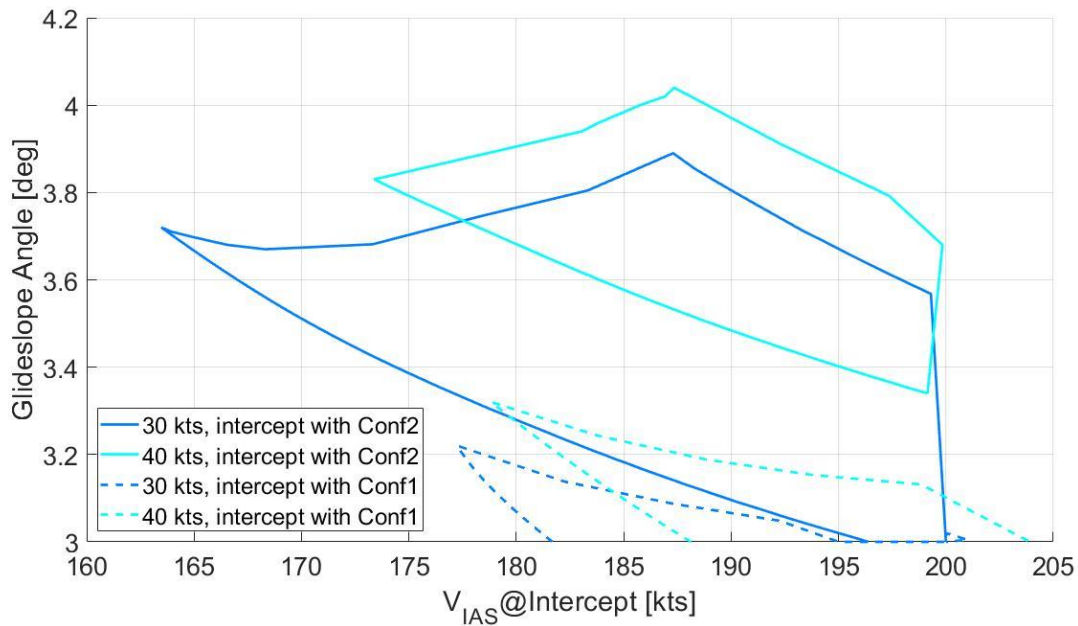


Figure 23: Influence of the wind on the speed envelope for A320 (aircraft mass 55 t, intercept altitude 3,000 ft) – intercept with Config1 and Config2.

4.3 Airbus A321

For the Airbus A321, a trimmed polar model is used for evaluation of aerodynamics and idle thrust. The A321 shows much higher maximum achievable glideslope angles than the A319 and A320. This can be explained by fact that the A321 possesses different engines and a different highlift system as the A319 and A320. However, the general shape and the influences of the parameters aircraft mass, intercept altitude and wind on the shape of the energy envelope is the same as for the A319. For a detailed description and explanation of the figures the reader should refer to section 4.1.

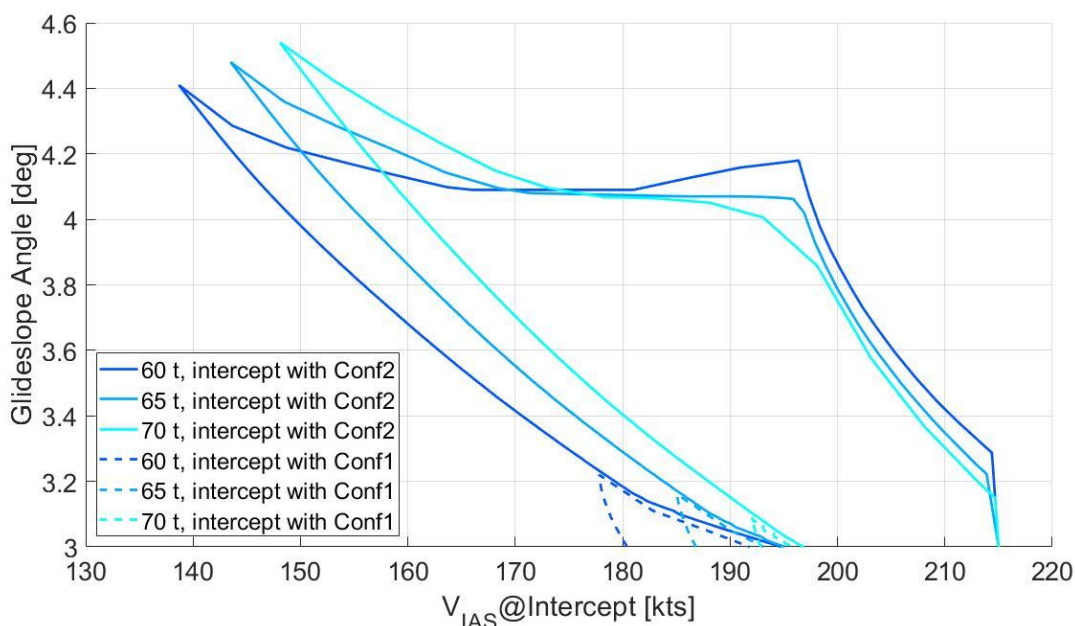


Figure 24: Influence of the aircraft mass on the speed envelope for A321 (intercept altitude 3,000 ft, no wind).

The influence of the intercept altitude as depicted in Figure 25 generally shows a similar shape of the energy envelopes compared to those seen before for the A319 and A320. However, interestingly the A321 is limited in terms of intercept altitude for energy-efficient approaches. Figure 25 shows an energy envelope for glideslope intercept at 2,000 ft and intercept with flaps in Config 2. A second envelope for intercepts with Config 1 (as seen for the intercept altitude of 3,000 ft) does not appear here. This is caused by the fact that the minimum possible airspeed with Conf 1 is too high and the deceleration rate with Conf 1 is too low to decelerate the aircraft to final approach speed within the remaining distance with an intercept altitude of 2,000 ft. For this very low intercept altitude of 2,000 ft energy-efficient approaches are only feasible when the glideslope is intercepted with flaps in Config 2. For an intercept altitude of 3,000 ft, however, Figure 25 shows an envelope for intercept with Config 2 and a small envelope for intercept with Config 1.

Interestingly, there is no envelope for intercept at higher altitudes (4,000 ft or 5,000 ft) as shown for the A319 and A320. This is caused by the fact that with these intercept altitudes energy-efficient approaches are just not possible with the A321 and the given aircraft mass of 65 tons and without wind. Due to the greater deceleration ability of the A320 (in comparison to the A319 and A320) the final approach speed is always reached before reaching 1,000 ft when the glideslope is intercepted with flaps in Config 2.

Apparently, aircraft with a better ability to decelerate should intercept the glideslope at lower altitudes rather than at higher altitudes. This is a very interesting outcome.

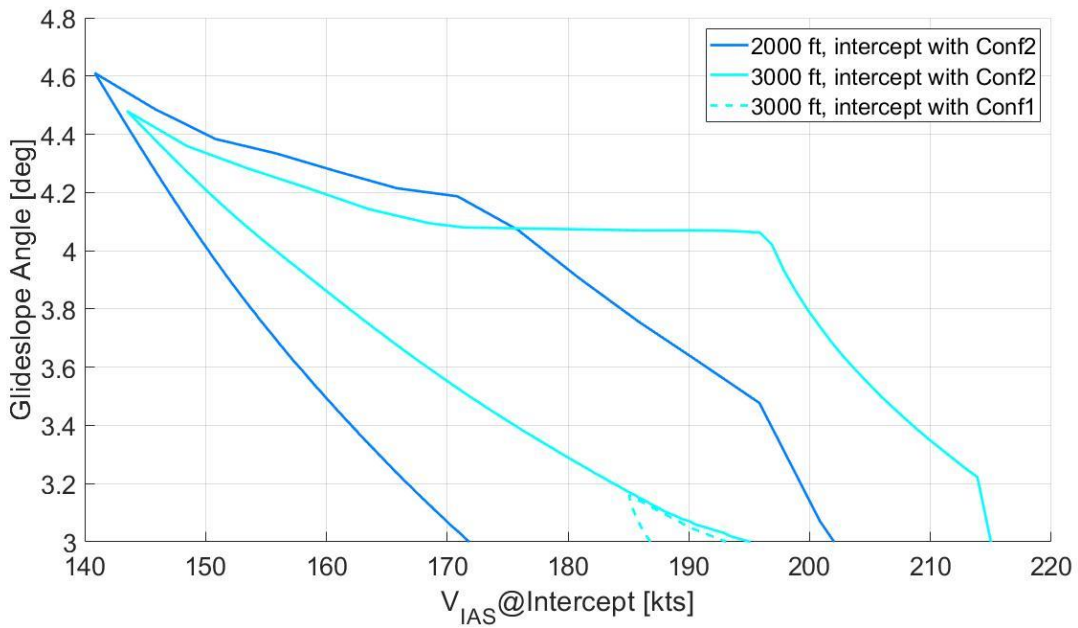


Figure 25: Influence of the intercept altitude on the speed envelope for A321 (aircraft mass 65 t, no wind).

The influence of the wind speed on the energy envelopes again show the same characteristics as described above in section 4.1 for the A319 only with higher maximum possible glideslope angles.

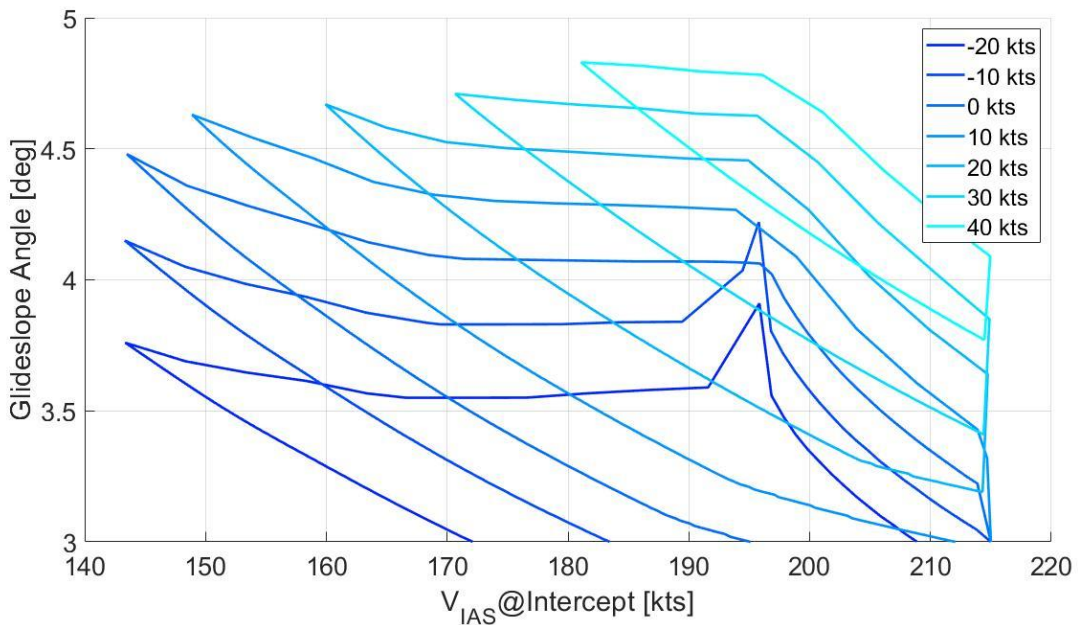


Figure 26: Influence of the wind on the speed envelope for A321 (aircraft mass 65 t, intercept altitude 3,000 ft) – intercept with Config2 only.

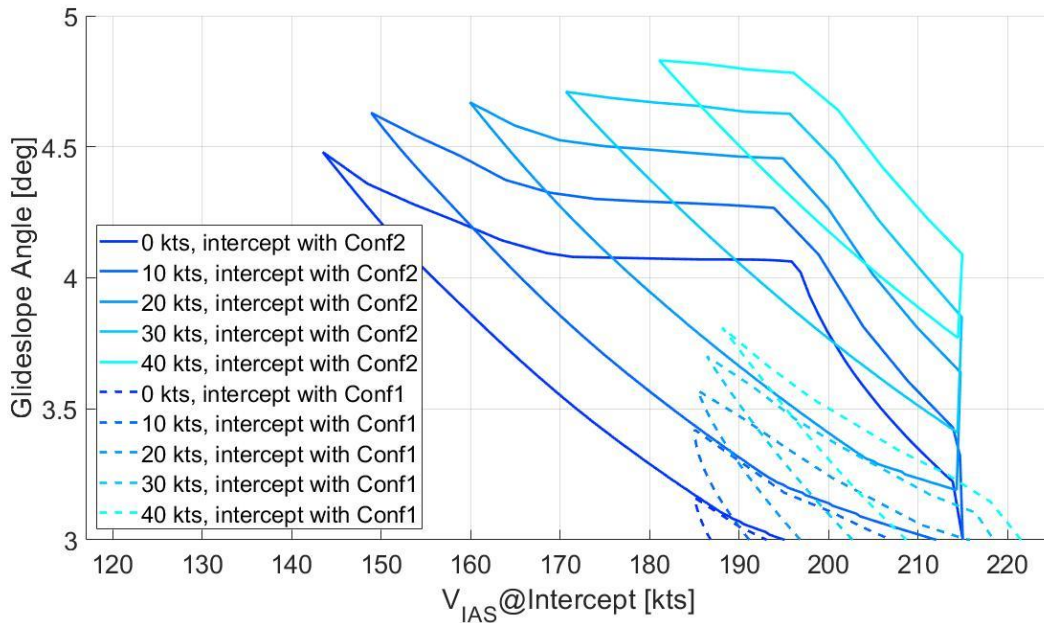


Figure 27: Influence of the wind on the speed envelope for A321 (aircraft mass 65 t, intercept altitude 3,000 ft) – intercept with Config1 and Config2.

4.4 Airbus A320 family comparison

An interesting comparison is the comparison of the different members of the A320 family. Figure 28 outlines the energy envelopes of the A319, A320 and A321 for an aircraft mass of 60 tons. This comparison is maybe not fully fair, as an A319 with 60 tons is a fairly heavy one (60 t = 88 % MTOW for A319), whereas an A321 with 60 tons is relatively light (60 t = 64 % MTOW). However, a comparison e.g. with the same percentage of the MTOW does not change the overall picture, that is obvious in Figure 28.

Figure 28 shows the significantly larger energy envelope of the A321 in comparison to the A319 and A320. While the envelopes of the A319 and A320 look similar like the change of the envelope with a mass variation, as observed in the subsections before, the energy envelope of the A321 looks totally different. One can observe the much larger maximum glideslope angle that can be achieved with the A321. Also, it is obvious that the A321 features a small additional envelope for intercepts with Conf1 (which is not feasible for A319 and A320).

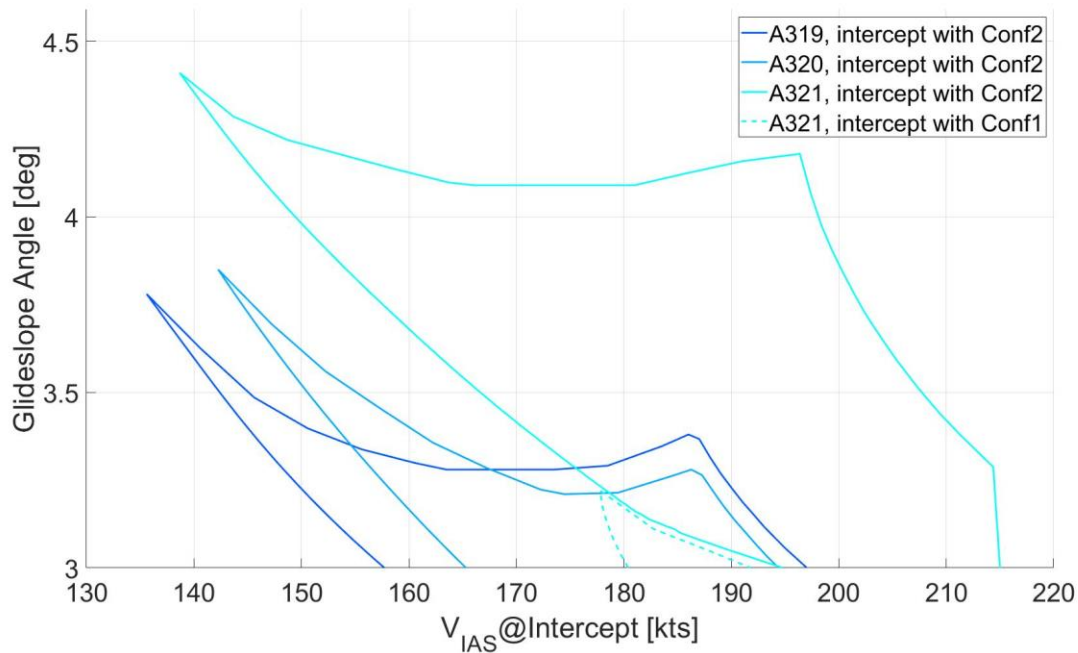


Figure 28: Comparison of A320 family at same conditions (aircraft mass 60 t, intercept altitude 3,000 ft, no wind).

The differences observed in Figure 28 between the A319 and A320 on the one hand side and the A321 on the other, can be explained by the different thrust ratings of the engines and by the fact that the A321 features a different high-lift system than the other two aircraft types. These facts cause different aircraft performance, hence different aircraft characteristics for IGS.

4.5 Boeing B787-9

For the Boeing aircraft, no trimmed polar model was available. For this reason, the ANP model is used here for the evaluation of aerodynamics and idle thrust.

Through the fact that the aerodynamic model of ANP features a single, speed-independent lift-to-drag-ratio for each flap configuration, the aircraft mass has no influence on the shape of the energy envelope. This can be clearly observed in Figure 29. The slight differences in the envelopes only stem from computational errors. Also, the usage of a constant lift-to-drag-ratio for each flap setting results in a cancelling of the belly-like shape of the upper boundary of the envelope. As the speed has no influence on the drag with the ANP model, the upper boundary is flat and not curved as with a more realistic trimmed polar model.

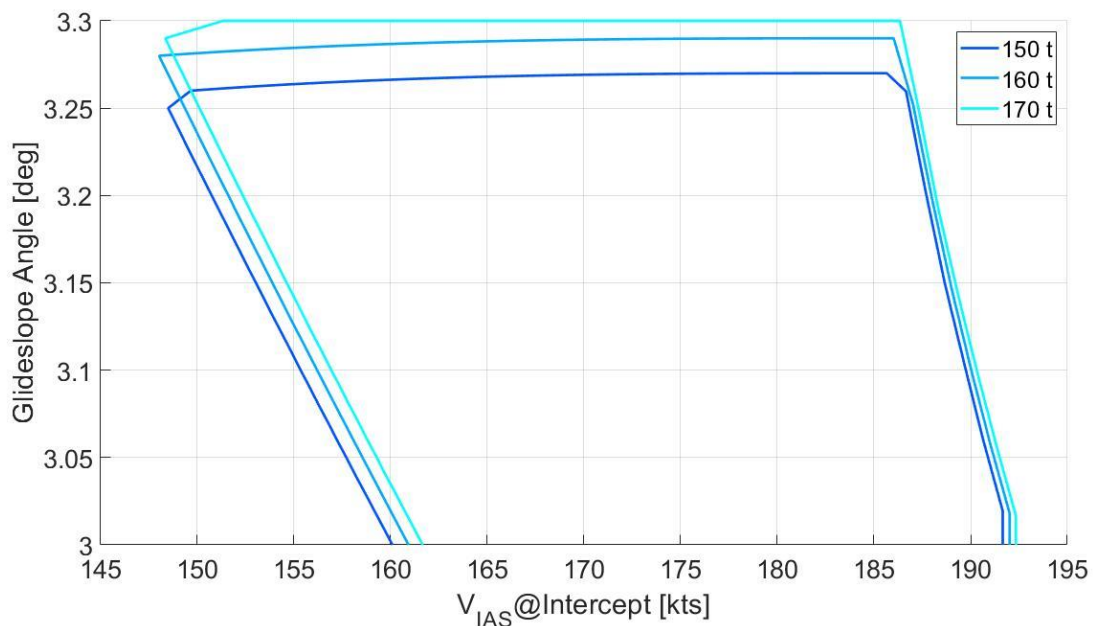


Figure 29: Influence of the aircraft mass on the speed envelope for B787-9 (intercept altitude 3,000 ft, no wind).

As explained above the variation of the aircraft mass does not make sense when using the ANP model. The variation of the intercept altitude, however, shows the same general trend, which was observed already before. Figure 30 shows that with increasing intercept altitude the envelopes shrink in size and move towards higher intercept speeds.

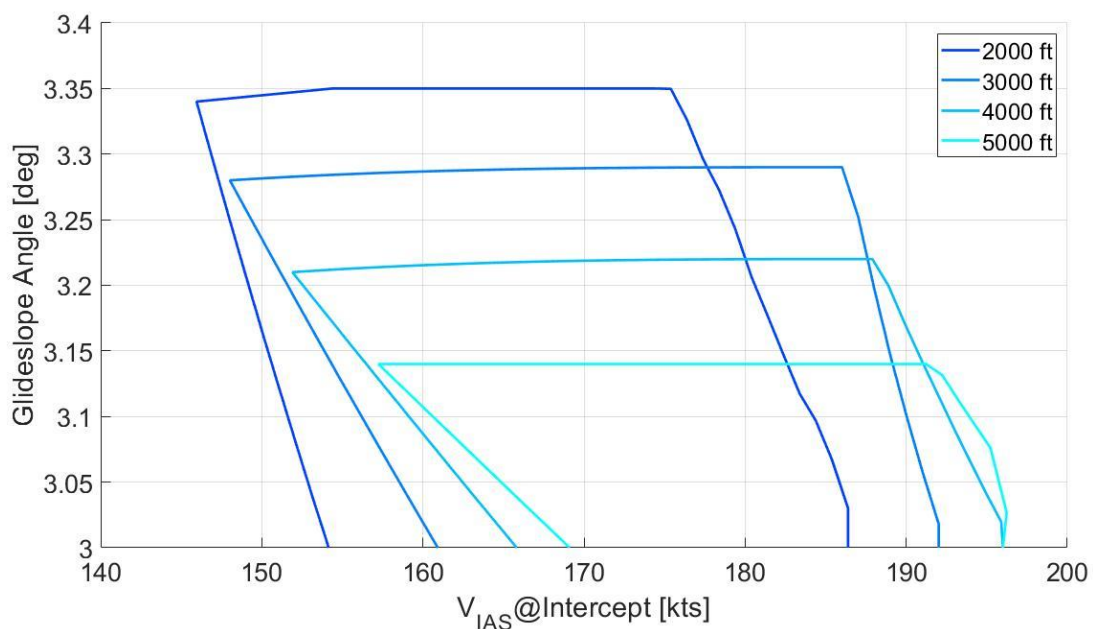


Figure 30: Influence of the intercept altitude on the speed envelope for B787-9 (aircraft mass 160 t, no wind).

Also the wind shows a comparable influence on the shape of the energy envelopes.

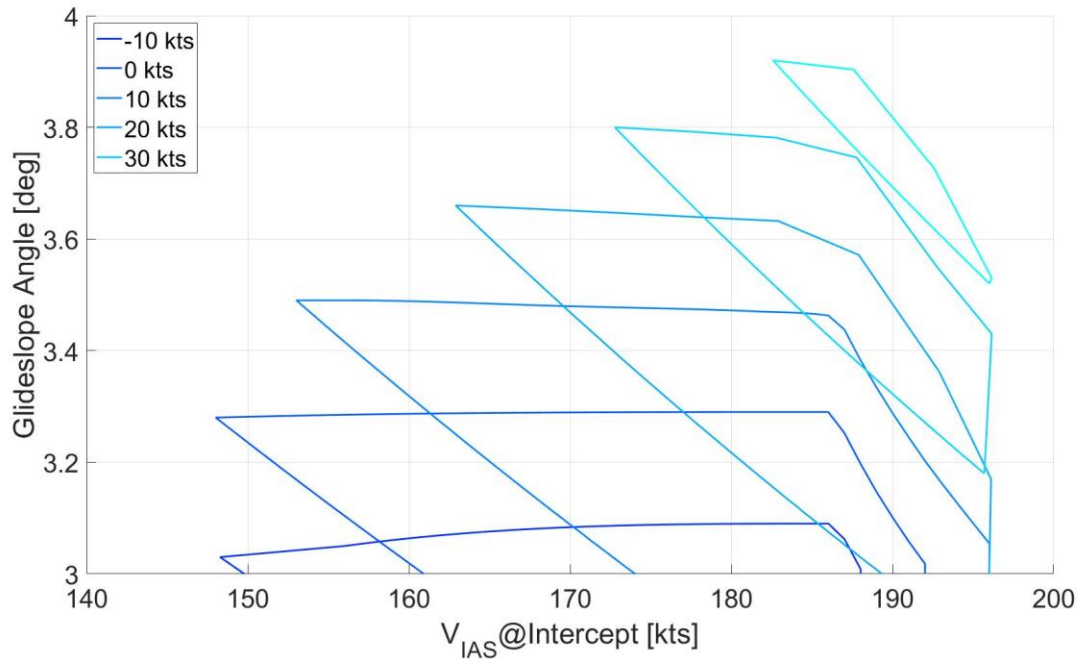


Figure 31: Influence of the wind on the speed envelope for B787-9 (aircraft mass 160 t, intercept altitude 3,000 ft).

Generally, the evaluation of energy envelopes for the B787 shows that the maximum glideslope angles, that are achievable in an energy-efficient manner, are in the same range as observed for the A320 family.

4.6 Influence on Fuel Consumption and Noise

Within the energy envelope all approaches can be considered energy-efficient. However, fuel consumption and also noise emissions vary within the envelope. Figure 32 shows the distribution of fuel consumption during final approach within the energy envelope for one example case of the Airbus A320 with a gross weight of 55 t, an intercept altitude of 3,000 ft and no wind. The fuel consumption outlined in Figure 32 is derived between glideslope intercept and touchdown.

One can observe in Figure 32 that the fuel consumption decreases with increasing intercept speed and with increasing glideslope angle, leading to the lowest fuel consumption in the upper right corner of the envelope and the highest fuel consumption in the lower left corner.

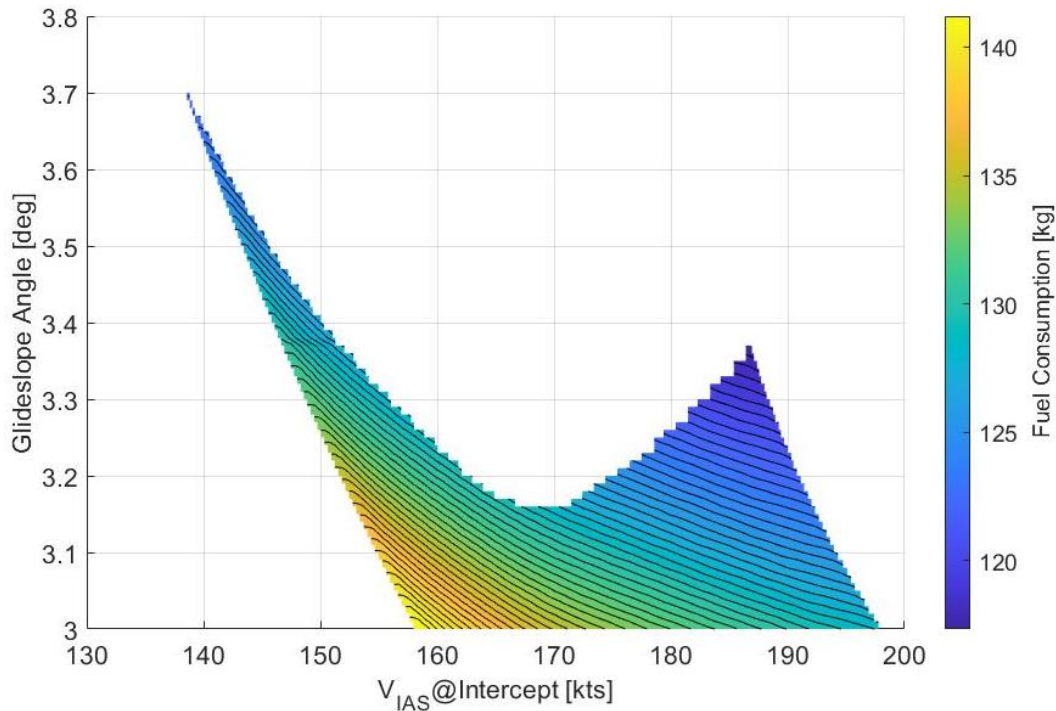


Figure 32: Fuel consumption during final approach within the energy envelope (A320, aircraft mass 55 t, intercept altitude 3,000 ft, no wind).

The reader should be aware, that the reduction of fuel consumption only stems from a smaller flying time between glideslope intercept and touchdown. In all approach cases shown in the envelope the engines are in idle until reaching 1,000 ft above ground, hence the fuel-burn in kg/s is always the same until that point. Also, below 1,000 ft above ground the final approach speed is the same for all approach cases shown in the energy envelope as the aircraft mass, wind etc. are the same for all approaches. Therefore, the fuel-burn in kg/s below 1,000 ft above ground is also the same for all cases, except that it is higher than the idle fuel flow. With increasing intercept speed the flying time from glideslope intercept to touchdown decreases, which directly saves fuel. The increased glideslope angle has a similar effect on the fuel burn, as with the same intercept altitude the glideslope intercept point moves towards the runway. This way, the flying time from glideslope intercept to touchdown decreases with increasing glideslope as well.

The values for fuel consumptions discussed before only concern the flight segment from glideslope intercept until touchdown. In any case, an approach with a faster intercept speed requires a later top of descent and therefore consumes more fuel on cruise level. However, the effects compensate each other when the fuel consumption of approaches with fast and low intercept speed are compared from the same point in front of both tops of descent. Figure 33 shows that an approach with a faster intercept speed still consumes less fuel than one with a smaller intercept speed, even when the whole fuel consumption from a fixed point before the top of descent to touchdown is considered (here 140 NM in front of the runway). In the exemplary case shown in Figure 33 the approach with the highest intercept speed consumes about 5.3 kg less fuel between glideslope intercept and touchdown than the approach with the lowest intercept

speed. From 140 NM in front of the runway to the threshold the difference in fuel consumption between both approaches is about 7 kg.

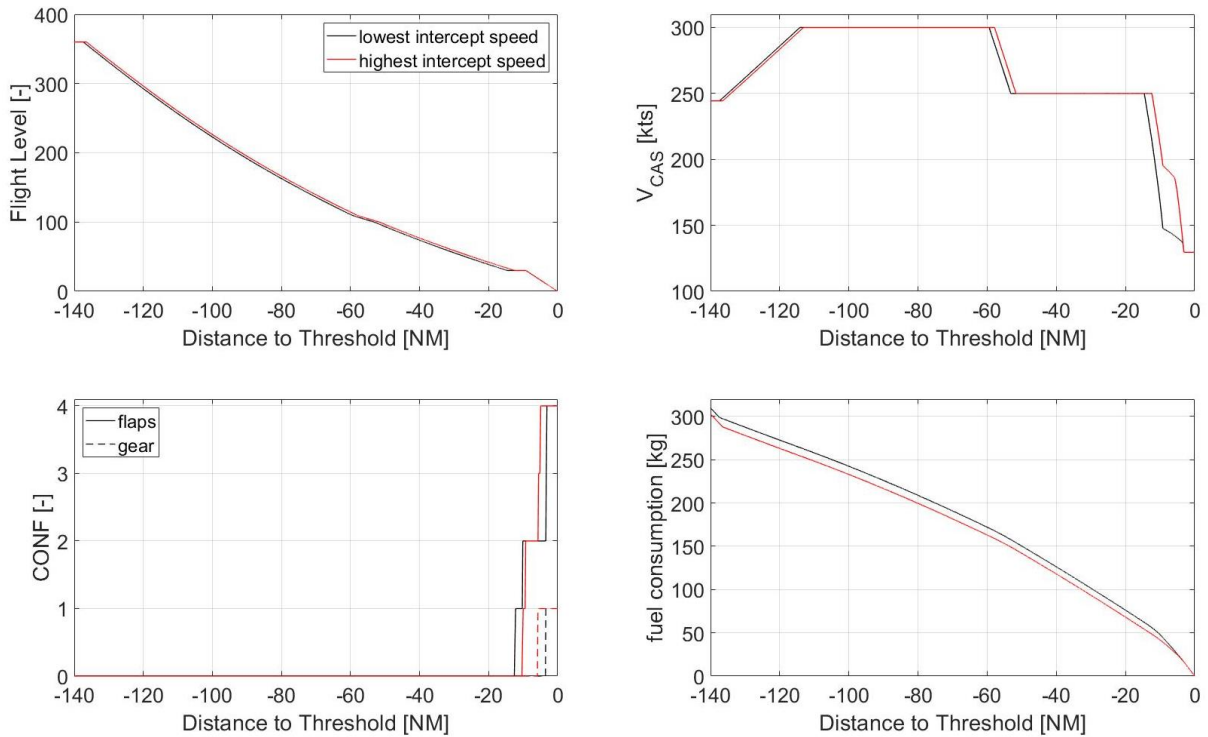


Figure 33: Exemplary approach from top of descent with lowest and highest glidepath intercept speed (A320, aircraft mass 55 t, intercept altitude 3,000 ft, no wind).

Fuel consumption is only one factor of a flight's environmental impact that varies within the energy envelope. Also, noise is affected by the intercept speed and the glideslope angle. No quantitative results on noise within the energy envelope will be presented here. However, some qualitative conclusions shall be made.

Generally, the approaches with a higher intercept speed should be louder than those with lower intercept speeds. The reason for this is, on the one hand, the faster airspeed, which results in more airframe noise by itself and, on the other hand, the necessity to configure the aircraft earlier with higher intercept speeds, which results in higher noise levels at least in some regions below the glidepath. Apart from this, an increase of the glideslope angle should generally reduce the noise perception on ground because of the higher altitude of the aircraft over a given point in front of the runway. This benefit is at least partly compensated by the necessity to configure the aircraft earlier with higher glideslope angles. Given the same intercept speed, a higher glideslope angle requires an earlier configuration of the aircraft because of the lower ability of the aircraft to decelerate. Nevertheless, past noise assessments for increased glideslope angles revealed that there is still a net benefit in terms of noise, even if an earlier configuration of the aircraft is considered [3]. Approaches with higher glideslope angles should therefore be less noisy than those with lower glideslope angles.

These qualitative thoughts on noise show at least that the noise minimum within the energy envelope is probably not in the same area as the minimum of the fuel consumption. Presumably, the noise minimum lies somewhere in the upper left part of the energy envelope, whereas the one of the fuel consumption lies in the upper right corner. Therefore, it can be expected that the final approach cannot be optimized with respect to both noise and fuel consumption, but that these parameters have to be traded against each other.

4.7 Business Jet

In order to support the flight trials performed in the project it would have been desirable to evaluate the energy envelopes also for business jets.

Unfortunately, no usable flight performance model for any kind of business jet was available. Also, the ANP database does not provide sufficient data of any business jet for the purpose described here.

Furthermore, within the project no flight data were available that could have been used for developing an own flight performance model of the business jets used in the project flight trials or for the verification of any other flight performance model.

For this reason, no energy envelopes could be evaluated for business jets. However, the flight physics are generally the same for aircraft, regardless the aircraft size. Therefore, the energy envelopes of business jets and their influences from parameters such as aircraft mass, wind etc. should be qualitatively comparable to the ones outlined here for bigger transport aircraft.

5 Conclusions

In order to assess the ability of modern transport aircraft to fly energy-efficient approaches with increased glideslope angles, energy envelopes have been evaluated by using a backwards simulation of idle approaches. The energy envelopes were evaluated for various aircraft types (A319, A320, A321 and B787-9). Two different types of aircraft performance model were used. For the aircraft of the A320 family a so-called trimmed polar model, which utilises trimmed drag polars and an accurate idle thrust model, was used. This model can be regarded as acceptably accurate. In case that no such model is available, the Aircraft Noise and Performance (ANP) database of Eurocontrol can be used as well. For the evaluation of the B737-800 and the B787 the ANP model was used. This model can be regarded as acceptably accurate for typical approach speeds and glideslope angles. For larger glideslope angles and non-typical approach speeds the accuracy of the ANP model is degraded.

The results of the approach calculations have been verified against real flight data and show an acceptable level of conformity. The verification was performed for the A320 (with a trimmed polar model) and B737-800 (with ANP) and for approaches with glideslope angles of 3° and 3.2° as only for these aircraft types and glideslope angles real flight data were available. The comparisons to the real flight data showed a sufficient accuracy. For this reason, it can be expected that the results are also acceptably accurate for higher glideslope angles and for other aircraft types, as long as the used performance model shows an acceptable accuracy. This might not be the case for the ANP model with large glideslope angles.

The parameters that influence the shape of the energy envelope, such as aircraft mass, glideslope intercept altitude or wind have been varied for the mentioned aircraft types in order to show the sensitivity of approaches with increased glideslope angles against these parameters.

The envelopes show that the influence of the aircraft mass on the maximum energy-efficiently achievable glideslope angle depends on the intercept speeds. While for high intercept speeds lighter aircraft can fly steeper approaches, heavier aircraft can fly steeper approaches at lower intercept speeds. The energy envelopes also show that it is favourable to have lower intercept altitudes at higher glideslope angles as a higher intercept altitude decreases the maximum energy-efficiently achievable glideslope angle. This especially applies to those aircraft types that show a good ability to decelerate without the use of airbrakes. The variation of wind reveals the strong influence of wind on the ability of aircraft to fly approaches energy-efficiently.

The analysis of fuel consumption within the energy envelope shows that the minimum fuel consumption is for approaches with large glideslope angles and high intercept speeds. Noise analysis was not performed here, but it can be expected that the minimum noise is not in the same region as the minimum fuel consumption. For this reason, it can be expected, that these two parameters have to be traded against each other.

The analysis of the variety of influencing parameters shows that for some aircraft types a kind of energy assistance system, which enables pilots to fly energy-efficiently even with increased

glideslope angles and under the various and changing conditions in real flight can be beneficial (such as the one developed by DLR called LNAS - Low Noise Augmentation System). Without such an assistance system the risk may rise that the increase of the glideslope angle will lead to a larger number of non-energy-efficient approaches, resulting in unnecessary noise immissions and/or fuel consumption.

6 References

- [1] N.N., SESAR ENV Assessment Process 4 (ERM methodology update), H2020 SESAR Project Environment support and coordination function, Deliverable D27, Edition 3.0, 12.05.2016.
- [2] <https://www.aircraftnoisemodel.org>
- [3] König, R. and Schubert, E., On the Influences of an Increased ILS Glide Slope on Noise Impact, Fuel Consumption and Landing Approach Operation, AIAC14 Fourteenth Australian International Aerospace Congress, 28. Feb. - 3. March 2011, Melbourne, Australia.